HHS Public Access

Author manuscript

Oncogene. Author manuscript; available in PMC 2016 May 18.

Published in final edited form as:

Oncogene. 2016 April 14; 35(15): 1926–1942. doi:10.1038/onc.2015.256.

Focal adhesion kinase-promoted tumor glucose metabolism is associated with a shift of mitochondrial respiration to glycolysis

Jianliang Zhang[1], **Qile Gao**[1], **Ying Zhou**[1], **Usawadee Dier**[2], **Nadine Hempel**[2], and **Steven N. Hochwald**[1,*]

[1] Department of Surgical Oncology, Roswell Park Cancer Institute, Elm and Carlton Streets, Buffalo, NY 14263.

[2] Nanobioscience Constellation, SUNY College of Nanoscale Science & Engineering Albany, NY 12203.

Abstract

Cancer cells often gains a growth advantage by taking up glucose at a high rate and undergoing aerobic glycolysis through intrinsic cellular factors that reprogram glucose metabolism. Focal adhesion kinase (FAK), a key transmitter of growth factor and anchorage stimulation, is aberrantly overexpressed or activated in most solid tumors including pancreatic ductal adenocarcinomas (PDACs). We determined whether FAK can act as an intrinsic driver to promote aerobic glycolysis and tumorigenesis. FAK inhibition decreases and overexpression increases intracellular glucose levels during unfavorable conditions including growth factor deficiency and cell detachment. Amplex glucose assay, fluorescence and carbon-13 tracing studies demonstrate that FAK promotes glucose consumption and glucose-to-lactate conversion. Extracellular flux analysis indicates that FAK enhances glycolysis and decreases mitochondrial respiration. FAK increases key glycolytic proteins including enolase, pyruvate kinase M2 (PKM2), lactate dehydrogenase and monocarboxylate transporter. Furthermore, active/tyrosine-phosphorylated FAK directly binds to PKM2 and promotes PKM2-mediated glycolysis. On the other hand, FAK-decreased levels of mitochondrial complex I can result in reduced oxidative phosphorylation (OXPHOS). Attenuation of FAK-enhanced glycolysis re-sensitizes cancer cells to growth factor withdrawal, decreases cell viability, and reduces growth of tumor xenografts. These observations, for the first time, establish a vital role of FAK in cancer glucose metabolism through alterations in the OXPHOS-to-glycolysis balance. Broadly targeting the common phenotype of aerobic glycolysis and more specifically FAK-reprogrammed glucose metabolism will disrupt the bioenergetic and biosynthetic supply for uncontrolled growth of tumors, particularly glycolytic PDAC.

*To whom correspondence should be addressed: Steven N. Hochwald, MD Professor of Oncology Dept. of Surgical Oncology Roswell Park Cancer Institute Elm and Carlton Streets Buffalo, NY 14263 Telephone: 716 845-3493 Fax: 716 845-1060 ; Email: steven.hochwald@roswellpark.org

Conflict of interest

The authors declare no conflict of interest.

Keywords

FAK; tumor metabolism; glycolysis; intrinsic factors

Introduction

Glycolysis maintains energy and carbon supply to meet high metabolic requirements during tumor growth and survival. Pancreatic ductal adenocarcinoma (PDAC) has a strong glycolytic phenotype.[1] Increased intracellular glucose levels have been observed in the majority of solid tumors including PDAC.[2-4] Based on this unique difference between normal and tumor tissues, attempts have been made to identify oncogenic glucose metabolic pathways and block glucose uptake in cancer cells. However, no effective therapeutic intervention targeting glucose metabolism in malignancy currently exists. An increased understanding of molecular events that are responsible for tumor-specific glucose elevation and usage will allow for effective targeting of glucose metabolism.

A dynamic balance of oxidative phosphorylation and glycolysis is essential for cellular adaptation to microenvironmental changes. Sustained elevation of intracellular glucose may favor the glucose-to-pyruvate reaction in tumor cells. In addition, the well-recognized finding of increased glycolysis in tumor cells results in excessive tumor lactate production.[5] Moreover, the transition from a localized-to-metastatic tumor phenotype is correlated with further increases in lactate efflux rate through overexpression of transporters including monocarboxylate transporter 4 (MCT4).[5] Elevation of glycolysis enzymes and transporters has been identified in various tumor types.

Growth factors including insulin and insulin-like growth factor 1 (IGF-1) stimulate glucose uptake and metabolism through receptor activation of FAK-related downstream signaling.[6-8] Abnormal hyperactivity of FAK due to gene amplification of FAK-associated signal transduction pathways promotes metabolic activity and proliferation even in the absence of growth factors. This notion is supported by the observation that FAK overexpression contributes to malignant cell glucose, lipid and amino acid metabolism.[9]

Although many oncogenes have been reported to modulate mitochondrial respiration, there is a paucity of information regarding a role for FAK in tumor glucose metabolism. A tumor suppressor, BTG2, inhibits tumor cell migration through interrupting mitochondria-related FAK-Src signaling.[10] FAK has been shown to translocate to the nucleus and interact with p53. This observation implies that FAK can serve as a “cortex to nuclear shuttle” to relay growth factor and anchorage stimulation for survival by p53-mediated mitochondrial-glycolytic balance. Furthermore, activation of FAK is associated with lactate dehydrogenase (LDH) release in nerve cells.[11] FAK contributes to MCT4-mediated migration and invasion of oral squamous cell carcinoma (SCC).[12] Although these observations imply a correlation between tumor-related FAK overexpression and lactate release, the direct link is still missing.

Our current studies have been performed to address several fundamental questions: 1) is FAK an intrinsic factor that promotes glucose elevation in PDAC cells? 2) Can FAK

modulate glucose-to-lactate conversion and efflux? And, 3) what are the key players in FAK modulation of oxidative phosphorylation (OXPHOS) and glycolysis in tumor cells. Our current observations demonstrate, for the first time, that FAK contributes to malignancy-related glucose elevation and conversion to lactate through direct interaction with key glycolytic proteins and via decreased mitochondrial complex I expression.

Results

Modulation of aberrant glucose elevation in PDAC cells

We analyzed the glucose content in human pancreatic ductal epithelial (HPDE) cells and four human PDAC cell lines. The steady-state levels of glucose in PDAC cells are 7-13 fold higher than that in HPDE (Fig 1A). Extracellular glucose is known to affect the levels of intracellular glucose in many cell types.[13] We adjusted the level of glucose in the KSFM medium used for HPDE cells to a similar level as in DMEM (Miapaca-2 cells), i.e. 4.5 g/l. The glucose levels in Miapaca-2 cells are significantly higher than in HPDE cells, when Miapaca-2 and HPDE are exposed to the same amount of extracellular glucose (Fig 1B). The results demonstrate that PDAC cells retain high levels of intracellular glucose, which is consistent with the phenomena that the majority of solid tumors accumulate intracellular glucose.

Next, we assessed the effects of extracellular stimuli on intracellular glucose levels. Growth factors and anchorage are essential extracellular stimuli to promote glucose metabolism and epithelial growth. Thus, we cultured Miapaca-2 cells on fibronectin-coated or uncoated ultra-low cell binding plate (anchorage) in the presence or absence of serum (growth factors). Interestingly, withdrawal of growth factors, anchorage, or both does not decrease but significantly increases intracellular glucose levels (Fig 1C). Therefore, in order to determine the intrinsic control of tumor cell glucose metabolism, most experiments are performed in growth factor and anchorage limited conditions. All values for lactate, glucose, and LDH have been normalized to protein content. The conditions for each experiment are documented in each figure legend.

Since normal (HPDE) and cancer cell lines (Mia, PANC, HS and Apsc-1) are typically cultured in different media (KSFM, DMEM, or RPMI), the levels of FBS, glucose, pyruvate, glutamine and other nutrients vary significantly. In order to examine the intrinsic cellular control of glucose metabolism in normal and PDAC cells, 2-NBDG [2-(*N*-(7-Nitrobenz-2-oxa-1,3-diazol-4-yl)Amino)-2-Deoxyglucose, a fluorescent glucose analog] was used to assess glucose influx under identical conditions, i.e. basic medium (DMEM) in the absence of FBS, pyruvate, and glutamine. PDAC-related glucose elevation is modulated by intrinsic factors but not nutrients (Fig 1D). The data supports the notion that oncogenic glucose elevation in PDAC cells is primarily controlled by intracellular or intrinsic factors.

FAK modulates intrinsic glucose levels

FAK relays both growth and attachment signals through its interactions with growth factor receptors and matrix proteins including fibronectin and integrins. Amplification of the *FAK* gene frequently occurs in solid tumors, which results in FAK overexpression. First, we

examined whether glucose elevation in PDAC correlates with increased FAK expression. The level of FAK protein in Miapaca-2 cells was significantly higher than that in normal cells (Fig 2A). This suggests that FAK elevation is associated with increased levels of glucose in PDAC cells.

Next, we elucidated the role of FAK in oncogenic glucose elevation using specific gene manipulation. To establish the link between FAK and intrinsic tumor cell glucose elevation, we suppressed FAK expression in tumor cells using siRNA. Inhibition of FAK expression decreased glucose levels under stimulus-limited conditions (0.5% FBS and uncoated plates) (Fig 2B). To rule out the possibility that transfection-associated cell injury may contribute to the decreased glucose levels, we stably transfected Miapaca-2 cells with constructs expressing GFP or m**C**herry-tagged **N**-**t**erminal **F**AK (CNTF), the F1 subdomain of FAK. F1 binding to Y397 is known to prevent FAK activation/phosphorylation and Src recruitment.[14] Interestingly, ectopic overexpression of the FAK F1 subdomain in Miapaca-2 cells decreases the levels of FAK protein (insets of Fig 2C), suggesting that the F1 subdomain can act as a dominant-negative (DN) form of FAK. F1 inhibition of FAK leads to decreased levels of intrinsic glucose under extracellular stimulation-limited conditions (Fig 2C). Inhibition of FAK expression using siRNA or F1 techniques may have off-target effects on other signaling pathways. To overcome this obstacle, we delivered the vectors expressing FAK or GFP to FAK knockout (KO) SCC cells. The level of glucose in FAK-transfected cells is significantly higher than that in GFP-transfected cells (Fig 2D), demonstrating a direct effect of FAK on glucose elevation. Finally, we determined whether FAK contributes to oncogenic glucose elevation in addition to normal glucose levels by transfecting HPDE cells with FAK or GFP vectors. Ectopic expression of FAK induces a dramatic increase in the glucose level in HPDE cells, compared to the GFP-transfected cells (Fig 2E). These observations clearly demonstrate that FAK modulates intrinsic glucose elevation in PDAC cells.

FAK promotes glucose consumption

A possible advantage of PDAC cells maintaining intracellular glucose at a high level is to accelerate the use of glucose. To assess the utilization of glucose, we analyzed glucose content in cell-conditioned and non-conditioned medium under identical conditions. The relative levels of glucose consumed by FAK KO SCC cells are significantly lower than that by the cells expressing wild-type (WT) FAK (Fig 3A). Furthermore, ectopic overexpression of FAK in HPDE cells promotes glucose consumption (Fig 3B), suggesting that FAK elevation can contribute to excessive utilization of glucose. Next, we determined whether interruption of the *FAK* gene in fibroblasts, normal cells with high metabolic activity, could reduce glucose consumption. We cultured FAK KO and WT FAK MEFs in DMEM medium for 48 hr. The relative level of glucose consumed by WT FAK MEFs is higher than that by FAK KO MEFs (Fig 3C), indicating that FAK is associated with glucose utilization in metabolically active cells.

Many factors such as the rates of uptake, influx, and metabolism affect the steady-state levels of intracellular glucose. However, increased uptake is essential for rapidly growing cells to fuel excessive glucose utilization. We utilized a fluorescent-tagged sugar, 2-NBDG,

to trace glucose influx. Interruption of the *FAK* gene in MEFs leads to a shift of fluorescence intensity to left (KO cells, the red line), i.e. lower levels of 2-NBDG, compared to WT FAK cells (the black line), demonstrating FAK-increased glucose influx (insets in Fig 3D). The relative level of 2-NBDG accumulating in FAK KO MEFs is significantly lower than that in the cells expressing WT FAK (Fig 3D). To elucidate the role of PDAC-associated FAK elevation in glucose influx, we have disrupted *FAK* gene expression in Miapaca-2 cells using the CRISPR-Cas9 genome editing system for *FAK* (Genecopoeia).[15] This is an all-in-one vector containing CRISPR Cas9 nuclease, one CRISPR sgRNA, the neo gene for G418 selection, and mCherry as a fluorescent reporter. Genome average copy numbers are often increased in tumor cells (https://cansar.icr.ac.uk; canSAR, Cancer Research UK). Transfection of PDAC cells (Miapaca-2) with CRISPR-Cas9 FAK constructs (CR-FAK) decreases but does not completely eliminate FAK expression (insets, Fig 3E). Nevertheless, reduction in *FAK* gene copies in the transfected PDAC cells decreases 2-NBDG uptake (Fig 3E). Furthermore, FAK expression in the CRISPRCas9-transfected Miapaca-2 cells has been restored through delivery of pcFAK (FAK, a construct of mCherry-tagged FAK) or pGFP (GFP, vehicle). Restoring FAK expression increases 2-NBDG uptake in Miapaca-2 cells (Fig 3F).

The glucose transporter (Glut1) contributes to the low level basal glucose uptake that sustains respiration in all cells. To examine the effects of FAK on Glut1 expression, the levels of Glut1 protein in Miapaca-2 cells expressing GFP (control) or CNTF (the FAK F1 subdomain) were assessed. The relative level of Glut1 in CNTF-transfected Miapaca-2 cells is lower than that in GFP-transfected cells (Fig 3G). Furthermore, CRISPR-Cas9 vector-disrupted *FAK* gene leads to decreased levels of Glut1 protein in Miapaca-2 cells (Fig 3H). To restore FAK expression, we have transfected FAK KO SCC cells with pGFP or pcFAK constructs. The level of Glut1 protein in FAK-reinstated cells (FAK) is higher than that in vehicle-transfected cells (GFP, Fig 3I). These results suggest that FAK-increased Glut1 levels can contribute to elevation of glucose uptake.

Our studies on FAK gene manipulation and glucose analysis demonstrate that FAK can promote glucose utilization, which is associated with increased glucose influx. This can provide a carbon source to fuel uncontrolled cancer cell proliferation under growth factor and/or anchorage stimulation-limited conditions.

FAK increases lactate production

FAK-induced fast turnover of glucose may lead to rapid pyruvate-to-lactate conversion. We assessed the amount of lactate released per hour to the medium by normal and PDAC cells. Cell homogenates as well as medium conditioned with HPDE and Miapaca-2 cells were subjected to de-proteinization and lactate analysis. Indeed, Miapaca-2 cells secrete significantly more lactate into medium than the HPDE cells (Fig 4A). Interestingly, the level of intracellular lactate in Miapaca-2 cells is also higher than in HPDE cells (Fig 4B). Lactate derived from glycolysis can be converted back to pyruvate for the TCA cycle. When mitochondrial respiration is limited to processing excessive pyruvate, intracellular lactate levels can be increased causing feedback inhibition of glycolysis. Cellular lactate secretion can remove the feedback inhibition of glycolysis. Increases in intracellular lactate levels (L)

and lactate release to the medium (M) suggest enhanced lactate metabolism in Miapaca-2 cells.

Next, we elucidated the role of FAK in aberrant lactate elevation. The level of lactate released into the medium conditioned with Miapaca-2 cells treated with the FAK kinase inhibitor, PF4554878, is significantly lower than that in DMSO-treated cells (Fig 4C). PF4554878 or defactinib is a potent and specific inhibitor of FAK currently being studied in a variety of solid tumors in clinical trials (https://clinicaltrials.gov/).[16] This drug has been shown to inhibit FAK activity in the low nanomolar range.[16] Secondly, CRISPR-Cas9 disruption of the *FAK* gene in Miapaca-2 cells leads to reduced lactate release, and restoration of FAK expression in the CRISPR-Cas9-trasnfected cells increases lactate release (Fig 4D). In addition, CRISPR-Cas9 disruption of the *FAK* gene reduces the level of intracellular lactate (Fig 4E, the left two bars), and forced FAK expression restores the lactate level in the CRISPR-Cas9 transfected Miapaca-2 cells (Fig 4F, the left two bars). Pyruvate is a key glycolytic product. Addition of pyruvate to the medium prevents decreased lactate levels associated with FAK deficiency (Figs 4E and 4F, the right 2 bars). This supports the notion that FAK can contribute to elevated glycolysis in PDAC cells since lactate-induced acidification is a hallmark of glycolysis. Thirdly, interruption of the *FAK* gene in SCC cells significantly decreased lactate release and intracellular lactate levels (Figs 4G & 4H). Finally, interruption of FAK expression in MEFs significantly decreased lactate secretion (Fig 4I).

Carbon-13 (^{13}C) labeling and magnetic resonance (NMR) analysis were performed to evaluate the role of FAK in glucose-to-lactate conversion. Miapaca-2 cells expressing the *GFP* (control) or the *CNTF* (the FAK F1 subdomain) gene were incubated in medium containing 4.5 g/l ^{13}C-glucose. The levels of ^{13}C lactate and ^{13}C glucose in the cell-conditioned medium were subjected to ^{1}H NMR analysis, and the ratios of lactate/glucose levels relative to the internal standard were calculated. A known pattern of ^{13}C-related split peaks of ^{1}H lactate is observed in the NMR profile (upper panel J). The ratio of lactate/glucose in control Miapaca-2 cell-conditioned medium (GFP) is higher than that in FAK deficient cell-conditioned medium (CNTF) (Fig 4J). This demonstrates that FAK contributes to glucose-to-lactate conversion in Miapaca-2 cells since a lower ratio in CNTF cell-conditioned medium indicates that less ^{13}C glucose is converted into lactate. To directly examine the effects of FAK on glucose-to-lactate conversion, ^{13}C NMR was performed to assess the ^{13}C lactate and glucose levels (upper panel K). CNTF inhibition of FAK in Miapaca-2 cells decreased the ratios of lactate/glucose (Fig 4K), indicating a role of FAK in glucose-to-lactate conversion. These observations support a vital role of FAK in modulation of glucose-to-lactate conversion in PDAC cells, indicating accelerated glycolysis.

FAK-enhanced glycolysis is associated with increases in key regulatory proteins

Glucose can be processed via two major pathways: glycolysis (acidification) and OXPHOS (oxygen consumption). To monitor FAK-modulated lactate efflux, we performed Extracellular Flux Analysis (Seahorse Bioscience) on stably transfected Miapaca-2 cells expressing GFP or CNTF to assess extracellular acidification rate (ECAR, Fig 5A). Basal glycolysis is decreased in cells expressing CNTF. On the other hand, CNTF cells display a

significant increase in glycolytic reserve capacity, which is calculated as the difference between Oligomycin A induced ECAR and basal ECAR (Fig 5B). This suggests that WT (high FAK) Miapaca-2 cells undergo glycolytic flux closer to their maximal rate compared to cells that express CNTF.

To define the molecular events that lead to FAK-enhanced glycolysis, we performed Western blot analysis and observed increases in several key regulatory proteins related to lactate production and transportation. CNTF suppression of FAK expression leads to decreased levels of enolase (ENO) in Miapaca-2 cells (the left panel, Fig 5C). Furthermore, CRISPR-Cas9 disruption of the *FAK* gene in Miapaca-2 cells decreases ENO protein levels (the right panel, Fig 5C). These observations suggest that aberrant conversion of 2-phosphoglycerate to phosphoenolpyruvate contributes to the glycolytic phenotype of PDAC. Indeed, high levels of enolase protein have been detected in samples from PDAC patients and cell lines.[17]

PKM2, converting phosphoenolpyruvate into pyruvate, is overexpressed in PDAC.[1] CNTF inhibition of FAK reduces PKM2 levels in Miapaca-2 cells (the left panel, Fig 5D). Furthermore, ectopic expression of mCherry-tagged FAK (FAK) in FAK KO SCC cells increases PKM2 levels (the right panel, Fig 5D). The data support the notion that FAK modulates PKM2.

Pyruvate can be converted into lactate by LDH, an enzyme often overexpressed or hyperactivated in PDAC.[18] CNTF inhibition of FAK decreases LDH levels in Miapaca-2 cells (the left panel, Fig 5E), and ectopic expression of FAK increases LDH levels in FAK KO SCC cells (the right panel, Fig 5E), indicating a correlation between FAK overexpression and LDH elevation. To verify the specificity of FAK-increased LDH activity, FAK expression was restored in FAK KO SCC cells, resulting in significantly enhanced LDH activity (Fig 5F). In addition, disruption of the *FAK* gene in MEFs significantly decreased LDH activity (Fig 5G). The results suggest that FAK contributes to LDH hyperactivity.

Lactate transported by MCT protein across the cell membrane sustains fast turnover of glucose-to-lactate, and MCT is involved in tumorigenicity.[5, 12] We elucidated the role of FAK in modulation of MCT expression. The relative levels of MCT1 protein in Miapaca-2 cells are higher than that in HPDE cells (the left panel, Fig 5H). Miapaca-2 cells expressing CNTF have less MCT1 protein than cells overexpressing GFP or FAK (the middle panel, Fig 5H). Furthermore, CRISPR-Cas9 interruption of the *FAK* gene in Miapaca-2 cells decreases MCT1 protein levels (the right panel, Fig 5H). Ectopic expression of FAK in CRISPR-Cas9-transfected cells leads to increased levels of MCT1 (the right panel, Fig 5H). FAK-increased MCT1 mass can increase the capacity of lactate flux during the high turnover of glucose to lactate in Miapaca-2 cells.

FAK interacts with PKM2

PKM2 is exclusively re-expressed in malignancies and promotes incorporation of glucose metabolites into macromolecules rather than burning metabolites to produce CO_2. Recently, it has been shown that the phosphotyrosine-binding function of PKM2 is required for cancer cell growth.[19] PKM2 binding with phosphotyrosine peptides via K433 disassociates its

tetramers to form pro-glycolytic monomers/dimers.[19] Sequence analysis of the FAK peptide reveals a putative PKM2 binding motif ($DDY_{397}A$) within the kinase active site of FAK, which is identical to the residues located at the −2, −1, and +1 position of tyrosine within the optimal PKM2 binding peptide (P-M2tide).[19] Our IP/Western studies suggest that PKM2 can bind to active FAK *in vitro* (Fig 6A & 6B). Y397 phosphorylation indicates FAK activation. Indeed, the level of phospho-FAK at Y397 in Miapaca-2 cells was significantly higher than that in normal cells (Fig 6C).

Next, we determined whether tyrosine phosphorylation of FAK enhances FAK binding with PKM2. IP/Western (Fig 6D) and ELISA (Fig 6E) studies demonstrate that stimulation of Miapaca-2 cells with a potent phosphotyrosine phosphatase inhibitor (pervanadate) enhances FAK phosphorylation and interaction with PKM2. In addition, mutated FAK Y397A retains less PKM2 than WT FAK (Fig 6F). This suggests that Y397 contributes to FAK binding to PKM2. Furthermore, immobilized recombinant FAK binds with purified PKM2 in a dose dependent manner (Fig 6G). Anti-phosphotyrosine antibody mimics and phosphotyrosine-BSA inhibits PKM2 interaction with FAK, indicating that tyrosine phosphorylation enhances PKM2 binding with FAK (Fig 6G). The results demonstrate that active FAK directly binds to PKM2, which can contribute to FAK-enhanced aerobic glycolysis through modulation of the key regulatory protein, PKM2.

FAK inhibition of mitochondrial respiration through altered complex I subunits

Extracellular flux analysis was performed to assess oxygen consumption rate (OCR). Decreased levels of FAK protein in CNTF-transfected cells results in a significantly increased basal OCR, ATP dependent OCR (difference between basal OCR and oligomycin A inhibited OCR) and maximal FCCP induced OCR, relative to pGFP-transfected Miapaca-2 cells (Fig 7A & 7B). The results demonstrate that FAK overexpression can suppress mitochondrial respiration in Miapaca-2 cells.

The Mito-tracker green fluorescence probe, which is membrane potential sensitive, was used to examine the distribution of functional mitochondria in live cells. A widely distributed network of mitochondria is observed in HPDE cells, whereas mitochondria are located around nuclei in Miapaca-2 cells (Supplemental Figure 1A). The FAK inhibitor, PF-4554878, extends the mitochondrial network (insets, Fig 7C) and increases the level of active mitochondria in Miapaca-2 cells (Fig 7C). To elucidate the role of FAK in cellular mitochondrial distribution, we examined the patterns in WT, FAK KO, and FAK-reintroduced MEFs. The mitochondrial network in FAK KO MEFs spreads more to the cell edge compared to WT FAK MEFs (the first and second images of Supplemental Figure 1B). Ectopic overexpression of FAK in FAK KO cells induces shrinkage of the mitochondrial network (the third image of Supplemental Figure 1B). In addition, CNTF inhibition of FAK promotes extension of the mitochondrial network (Supplemental Figure 1C). These observations demonstrate that FAK can modulate the pattern of mitochondrial distribution, which can impact mitochondrial function and contribute to FAK-decreased oxygen consumption.

Mitochondrial complex I is the first enzyme of the electric transport chain and involved in tumorigenicity.[20] We determined whether FAK can modulate the protein levels of complex I

subunits NDUFA9 and NDUFB8. FAK elevation in Miapaca-2 cells is negatively correlated with NDUFA9 and NDUFB8 mass, compared to HPDE cells (Fig 7D). Interruption of the *FAK* gene in MEFs leads to increased levels of NDUFA9 and NDUFB8 proteins (Fig 7E). To verify FAK-decreased complex I subunit levels in tumor cells, WT and FAK KO SCC cell lysates (40, 20 and 10 μg protein/lane) were loaded and show that disrupted *FAK* gene expression increases NDUFA9 and B8 levels (Fig 7F). Next, we examined FAK modulation of complex I subunit expression in PDAC cells. CNTF inhibition of FAK increases NDUFA9 and NDUFB8 levels (Fig 7G). The band intensity of NDUFA9 in FAK deficient Miapaca-2 cells (CNTF-transfected) is much high than WT cells (Fig 7H). Furthermore, we used the CRISPR-Cas9 genome editing technique to disrupt the *FAK* gene in Miapaca-2 cells. FAK deficiency results in increases in both NDUFA9 and NDUFB8 protein mass in PDAC cells (Fig 7I). The results indicate that FAK can decrease complex I subunit levels. These findings are consistent with our analysis of mitochondrial function, i.e. downregulation of FAK expression leads to increased oxygen consumption.

FAK suppression restores the dependency of PDAC cells on growth factors and reduces tumorigenicity and tumor glycolytic proteins

Malignant cell elevation of FAK expression can maintain cell viability through intrinsic induction of glucose metabolism to compensate for the lack of anchorage and growth factor-stimulated glucose uptake. We determined whether suppressed FAK expression could restore the dependency of PDAC cells on growth factor stimulation. Miapaca-2 cells expressing the *GFP* or *CNTF* gene were cultured in medium containing 0-10% FBS for 24 hr and subjected to cell viability assay. The relative cell viability of CNTF-transfected Miapaca-2 cells is dependent on FBS doses; whereas FBS levels have minimal impact on GFP-transfected PDAC cells (Fig 8A). The *KRAS* gene is mutated in nearly all PDAC samples,[21, 22] and FAK is required for KRAS-driven tumorigenicity.[23] A colon cancer cell line with well characterized *KRAS* codon 12 mutation, HCT116, was stably transfected with the *CNTF* or *GFP* gene, cultured in medium containing 0-10% FBS, and subjected to cell viability assay. CNTF inhibition of FAK resensitizes *KRAS*-mutated HCT116 cells to growth factor stimulation (Fig 8A).

Following stable disruption of FAK expression, apoptosis and cell viability are unaltered when cells are cultured in normal media with full serum. In addition, apoptosis is slightly, but not significantly increased in FAK deficient Miapaca-2 cells grown in growth factor and anchorage limited conditions and stably transfected with CRISPR-Cas9 FAK constructs (relative levels of DNA fragmentation: 2.79 ± 0.06), as compared to controls (2.49 ± 0.18, p=0.19). However, in the growth factor and anchorage limited conditions, cell viability is significantly reduced following CRISPR-Cas9 *FAK* gene disruption and improved with FAK restoration as shown in Figure 8B. These are expected results as FAK depletion in anchorage limited conditions has been shown to result in reduced tumor cell growth.[24–26]

To determine whether FAK modulates glycolysis and tumorigenicity *in vivo*, we implanted GFP- or CNTF-transfected tumor cells into the right (GFP) and left (CNTF) mouse axilla, respectively. The protein levels of key glycolytic proteins including ENO1, PKM2, LDH, MCT1 and MCT4 in CNTF-transfected xenografts (FAK deficient) are lower than those in

GFP-transfected cells (Fig 8C). This suggests that FAK contributes to enhanced tumor glycolysis *in vivo*. The growth of tumors derived from GFP-transfected HCT116 cells is much faster than that from CNTF-transfected cells (Fig 8D). The weights (Fig 8E) and sizes (Fig 8F) of isolated tumors derived from GFP-transfected HCT116 cells is dramatically heavier and larger than that from CNTF-transfected cells, respectively. This demonstrates that FAK modulation of intrinsic glucose metabolism plays a key role in tumorigenicity.

These observations support the notion that FAK can act as an intrinsic factor to promote cell growth in a growth factor-independent manner through increased glycolysis and decreased OXPHOS (Fig 8G).

Discussion

Modulation of glucose elevation in PDAC cells

Our results demonstrate that PDAC-related intracellular glucose elevation is mediated through an intrinsic cellular factor. This notion is supported by the observation that changing extracellular glucose and stimulation (growth factors and extracellular matrix) does not lead to normalization of tumor cell glucose elevation. When normal and PDAC cells are cultured in their optimal medium, intracellular glucose levels in tumor cells are about 7 to 13-fold higher than that in normal cells. The glucose levels in Miapaca-2 cells are still twice that in normal cells, when they are exposed to the same levels of extracellular glucose. This is in line with the observation that intracellular glucose accumulates in colorectal tumors *in vivo.*[4] In addition, culturing Miapaca-2 cells under conditions with minimal growth and anchorage stimulation does not decrease intracellular glucose levels, indicating intrinsic factor control of glucose levels in Miapaca-2 cells.

FAK regulation of intracellular glucose levels

FAK is well accepted for its role in cell attachment and motility, which demands fast ATP turnover through glucose metabolism. Our data demonstrate that FAK overexpression increases intracellular glucose levels. In addition, transient and stable transfection, gene knockout, and restoration of FAK expression in fibroblasts, SCC cancer cells as well as normal pancreatic ductal and PDAC cells allows us to establish a key link between FAK control of intrinsic glucose elevation. FAK-increased intracellular glucose is associated with high glucose consumption and uptake in PDAC cells. FAK regulation of glucose transport activity has been observed in other types of cells.[27, 28] Rapid glucose influx can support enhanced glucose metabolism and retention of high levels of intracellular glucose. This may favor increased glycolysis in PDAC cells, which can fuel cell growth and accounts for the phenomenon that FAK elevation is common in localized and metastatic PDAC.[29, 30]

High levels of extracellular glucose can enhance FAK activity or phosphorylation.[31] Those observations support a role of FAK in the cell responding to extracellular glucose stimulation in normal cells. Aberrant activation of FAK through mechanisms including gain-of-function mutation such as *KRAS* mutation or amplification of oncogenes can mimic extracellular glucose stimulation and retain intracellular glucose at high levels in PDAC

cells. Indeed, the intracellular glucose levels in Miapaca-2 cells are higher than that in normal cells.

FAK enhancement of glycolysis and inhibition of OXPHOS

Many PDAC cells including Miapaca-2 have a glycolytic phenotype. Our data demonstrate that the pro-oncogene FAK can induce a shift of the glycolysis-OXPHOS balance towards glycolysis. Several lines of evidence support this notion. First, FAK enhances lactate production. Pyruvate can be converted to lactate in the cytosol or be processed via the TCA cycle/OXPHOS in mitochondria. FAK-increased lactate efflux and intracellular lactate elevation indicates rapid turnover of glucose to lactate via glycolysis. Second, CNTF inhibition of FAK in Miapaca-2 cells reduces acidification. Lactate release to the medium results in low pH. Therefore, low acidification rates of CNTF-transfected cells indicate low pyruvate-to-lactate conversion or glycolysis, suggesting a positive association between FAK expression and glycolysis. Finally, FAK inhibition leads to increased oxygen consumption. The mitochondrial electric transport chain takes oxygen to generate H_2O by oxidizing NADH to NAD. High oxygen consumption of CNTF transfected Miapapca-2 cells suggests that FAK inhibition can promote OXPHOS.

FAK-altered levels of lactate biosynthesis and mitochondrial respiration proteins

FAK overexpression in PDAC cells enhances lactate production through alterations of factors including ENO, PKM2, LDH, and MCT1, which are responsible for pyruvate-to-lactate conversion and lactate transport. ENO1 is overexpressed and phosphorylated in PDAC cells[32, 33] and has been shown to be an important prognostic factor for survival in patients with pancreatic cancer.[17] It has been reported that FAK-related signaling pathways contribute to LDH expression in endothelial cells.[34] Integrin-FAK signaling can contribute to MCT4-modulated migration and invasion of oral SCC.[12]

PKM2 binding to phosphotyrosine proteins is essential for cell transformation and growth through alterations of PKM2 conformation and activity. Interestingly, the residues of the FAK active site match the optimal PKM2 binding peptide that has been reported to trigger PKM2 conformation changes as well as promote glycolysis and proliferation.[19] IP/Western blot, ELISA with purified proteins, mutagenesis of FAK Y397 and phosphotyrosine phosphatase inhibition studies demonstrate that FAK directly interacts with PKM2. Therefore, FAK activation via Y397 phosphorylation can promote PKM2-increased glycolysis to fuel cancer proliferation. In addition, the phosphotyrosine peptides containing the *in vivo* SRC kinase site on ENO1 and LDH can bind to and alter PKM2 conformation.[19] Thus, FAK-modulated LDH and ENO1 levels can contribute to PKM2-promoted glycolysis in tumor cells.

FAK expression is negatively correlated with the levels of complex I subunits, which is associated with alteration of mitochondrial distribution and mass. This can contribute to FAK-decreased oxygen consumption in PDAC cells. On the other hand, FAK has been reported to modulate mitochondrial levels in muscle cells that predominantly rely on OXPHOS for ATP production. For example, it has been reported that FAK interacts with mitochondrial transcriptional regulators and enhances stretch-induced mitochondrial

biogenesis.[35] Swelled mitochondria in the myocardium of FAK KO mice imply a role of FAK in control of mitochondrial morphology and distribution.[36] FAK downregulation of complex I expression can contribute to the glycolytic phenotype of PDAC cells.

Summary and prospective view

Our current work demonstrates that pro-oncogenic FAK contributes to intrinsic glucose elevation in PDAC cells by shifting the OXPHOS-to-glycolysis balance (Fig 8G). The mechanism of action is likely in part due to direct binding of FAK to PKM2. Furthermore, FAK-promoted glycolysis and suppressed mitochondrial function are associated with increased ENO1, PKM2, LDH, and MCT mass and decreased mitochondrial complex I subunit expression. Aberrant FAK expression can sustain glucose metabolism to support tumor cell growth during growth suppressing conditions such as lack of growth factors. Disruption of FAK function restores the dependency of tumor cells on growth factors and reduces tumorigenicity. We speculate that small molecules targeting FAK control of tumor metabolism and survival and specifically the interaction of FAK and PKM2 may prevent growth and/or migration of PDAC, particularly malignancies with a glycolytic signature.

Materials and methods

Cell lines and reagents

Human PDAC cell lines (Miapaca-2, Panc-1, HS766T and Aspc-1 were obtained from the ATCC (Manassas, VA) and tested for mycoplasma contamination. HPDE cells were provided by Dr. Otay (University of North Carolina). WT FAK and FAK KO mouse squamous cell carcinoma cells were provided by Prof. Margaret Frame[26]. Recombinant full length FAK and the FAK FERM domain were purchased from Life Technologies (NY, USA) and Blue Sky Biotech (MA, USA), respectively. Recombinant FAK FERM-Y307A protein (Y397 substituted with alanine, A397) was provided by Tim Marlowe (Roswell Park Cancer Institute). Anti-ENO1 (#3810), anti-PKM2 (#4053), anti-FAK (clone 4.47, #05-537) and anti-phosphor-Y397 FAK (#3283) antibodies were from Millipore (MA, USA) or Cell Signaling Technologies (MA, USA). The antibodies recognizing GAPDH (#398600), the subunits of mitochondrial complex I, NDUFA9 (#459100) and NDUFB8 (#459210), were from Life Technologies (NY, USA). The antibodies recognizing LDH (SC-33781), glucose transporter 1 (Glut 1, SC-7903), lactate transporters, MCT1 (SC-365501) and MCT4 (SC-50329) were from Santa Cruz Biotechnology (CA, USA). An anti-β-actin (A5441) antibody was from Sigma (MO, USA). Glucose, lactate, and LDH assay kits were from Life Technologies and Sigma, respectively. WST-1 was from Roche (NY, USA). Chemical reagents were from Fisher Scientific (PA, USA). A specific FAK inhibitor, PF4554878, was provided by Pfizer (CT, USA).

Vector construction and expression

The mCherry-tagged FAK (pcFAK) was obtained from Addgene (MA, USA). The expression vector of the FAK subdomain (F1, amino acids: 1-126) was obtained by restriction enzyme cleavage between Eco RI and Not I, blunting ends and re-ligation of the rescued pcFAK to form the vector of pCNTF. Cells were transfected with pGFP, pcFAK, or

pCNTF and selected/maintained by culturing the transfected cells in the medium containing G418. CRISPRCas9 FAK constructs were purchased from GeneCopoeia (MD, USA).

Glucose assay

HPDE, Miapaca-2, PANC-1, HS766T, and Aspc-1 were cultured on a fibronectin-coated or non-coated low-cell binding 6-well plate in KSFM, DMEM, or RPMI 1640 medium in the presence or absence of 10% FBS for 24-48 hr. Medium and attached cells were harvested and subjected to Amplex Red glucose assay (Life Technologies, NY, USA). The protein levels in cell lysates were determined using BCA Protein Assay kit (Pierce, IL, USA). The amounts of glucose that were consumed by the cells were calculated by subtracting the amount of glucose in cell-conditioned medium from that of the medium without cell conditioning. Glucose levels were normalized to cellular protein levels and expressed as μg glucose/mg protein, i.e. the amount of glucose utilized by cells defined per amount of protein mass.

Immunoprecipitation (IP)/Western blot analysis

Full-length FAK (2 ng/μl, #PV3832, Life Technologies, USA) and active PKM2 (6 ng/μl, #6372, BioVision, CA, USA) in the binding buffer (0.05% BSA, 5 mM DTT, 0.05% Triton X100 and 1x PBS, pH 6.5) were mixed and incubated at 4°C for 1 hr. Then, anti-PKM2 antibody (#4053, Cell Signaling Biotechnology, MA, USA) or anti-FAK4.47 was added to the mixture and incubated at 4°C for 2 h. In addition, AG-agarose plus was added, and the mixture was incubated at 4°C overnight.

Immunoprecipitates or cell lysates in NP-40 lysis buffer containing protease and phosphoratease inhibitor cocktails (Roche, USA) were loaded, and gels run as previously described. [30, 37] Band intensities were quantified using Image-J software (NIH) and normalized to the levels of total FAK, GAPDH or β-actin intensity.

Glucose uptake assay

Cells were cultured in medium containing 0.5% FBS for 48 hr. Then, 5 μl of 2-NBDG (20 mM) was added to 1 ml of medium (final 2-NBDG concentration: 100 μM) and kept for 2 hr. Cells were detached from plates using Accutase (Fisher Scientific, USA), washed, and resuspended in 0.5 ml of PBS. Flowcytometry was performed on the Fortessa instrument. The representative histogram and the mean fluorescence intensity of 2-NBDG in the gated cells are shown. To determine glucose uptake that is specifically driven by intrinsic factors, cells on low cell binding wells were cultured in basic DMEM medium containing 100 μM 2-NBDG without FBS, glucose, pyruvate, and glutamine for 2 hr. The cells were rinsed in PBS and homogenized in lactate assay buffer. Fluorescence intensity and protein levels of cellular homogenates were determined.

Lactate assay

Cells on fibronectin-coated or no-coated plates were kept in stimulus-limited medium (0.5% FBS) for 48 hr. Medium and lysates derived from attached cells were collected and deproteinized with a 10 kDa MWCO spin filter to remove LDH. The lactate levels in medium and deproteinized cell lysates were measured using a lactate assay kit (Sigma).

Protein levels in the lysates that were retained on the filter were analyzed. The lactate levels were determined from the standard curve and normalized to the total cellular protein levels.

^{13} Carbon tracing and NMR analysis

GFP- or CNTF-transfected Miapaca-2 cells were kept in medium containing 4.5 g/l of ^{13}C-labeled glucose for 48 hr. The lactate in conditioned medium was extracted using perchloric acid (0.9M). The extracts were neutralized using KOH, freeze-dried, and dissolved in 0.8 ml of D_2O. Proton (^{1}H) and ^{13}C nuclear NMR were performed to determine lactate and glucose levels [The NMR Spectroscopy Facility, Roswell Park Cancer Institute (RPCI)]. Ethylene glycol was used as an internal standard to calculate the relative levels of lactate and glucose. The ratios of lactate/glucose were calculated for the assessments of glucose-to-lactate conversion.

Extracellular flux analysis of glycolysis and mitochondrial function

Seahorse $XF24_3$ Extracellular Flux Analyzer (Seahorse Bioscience, North Billerica, MA, USA) was used to assess the live cell OCR, an indicator of mitochondrial respiration; and the ECAR, an indicator of net proton loss during glycolysis. Cells (40,000 cells/well; optimized cell seeding number) were kept on the XF24 culture plate containing XF media (Seahorese Bioscience) in a non-CO_2 37°C incubator for 1 hr prior to OCR and ECAR measurements. Each measurement was taken for a 3 minute period, followed by 3 min mixing and re-oxygenation of the media. Three basal rate measurements were taken prior to injection of pharmacological manipulators of mitochondrial respiratory chain protein (Mitochondrial stress test). Following the establishment of basal OCR and ECAR readings, Oligomycin A (1μM) was injected to inhibit ATP synthase. Maximal respiration was achieved by exposing cells to the mitochondrial uncoupler carbonyl cyanide-ptrifluoromethoxyphenyl hydrazone (FCCP; 300nM). Antimycin A (1μM) was added to prevent all mitochondria-dependent OCR, by inhibition of mitochondrial complex III. Each cell line was represented in at least 4 wells per experiment and replicate experiments carried out at least three times. ECAR and OCR values were normalized against total protein per well. Basal mitochondrial OCR was derived by subtracting the third OCR reading from that following Antimycin A addition. Respiratory reserve capacity was calculated as the difference between maximal FCCP induced OCR and basal OCR. Glycolytic reserve was determined as the difference between Oligomycin A stimulated ECAR and basal ECAR.

LDH activity assay

Cells were cultured on fibronectin-coated or non-coated plates and kept in stimulus-limited medium (0.5% FBS) for 24-48 hr. Protein and lactate levels of cell lysates were determined using a LDH activity assay kit (Sigma). Serial measurements were made every 5 min. The changes from initial to final readings were used to calculate the amount of NADH generated by LDH in the samples. LDH activity was reported as nmole/min/ml/mg protein or milliunit (mU)/ml/mg. One unit of LDH activity was defined as the amount of enzyme that catalyzes the conversion of lactate into pyruvate to generate 1 μmole of NADH per minute at 37°C.

ELISA assay of FAK-PKM2 interaction

Full-length FAK (0.25 ng/μl in PBS, pH 7.4, #PV3832, Life Technologies, USA) or purified FAK FERM domain (amino acids 31-405) was immobilized on the wells of 8-well Immuno Module (MaxiSorp, #468667, Fisher Scientific, PA, USA) at 4°C overnight. The FAK-coated wells were rinsed with PBS (pH 6.5) and blocked with 10% BSA. Recombinant PKM2 (0-200 nM, #6372, BioVision, CA, USA) in the binding buffer containing 0.05% BSA, 5 mM DTT, 0.05% Triton X100 and 1× PBS, pH 6.5 was added to the FAK-coated wells and incubated at room temperature for 2 hr. Immunodetection was performed using an anti-PKM2 antibody (1:1000, #4053, Cell Signaling Biotechnology, MA, USA) in the buffer containing 20% Super Blocker and 1× PBS (pH 7.4), an anti-rabbit IgG secondary antibody (1:3000), and BM Blue POD Substrate (Roche, IN, USA).

Cell viability assay

pGFP-, pCNTF FAK-, pCRISPR-Cas9-, or pcFAK-transfected cancer cells were cultured on the wells containing 0-10% FBS for 24 hr. WST-1 was added to the wells. The 96-well plate was kept in a 37°C incubator for 10-30 min, and then the absorbance at 450 nm wave length was determined on a microplate reader.

Xenograft mouse models

SCID mice were obtained from the Laboratory Animal Resources at RPCI. Animal experimental protocols were approved by the RPCI-Institutional Animal Care and Use committee. HCT116 cells (1.5×10^6 cells, 100 μl/mouse) expressing the *GFP* or *CNTF* gene were mixed with 50% Matrigel Matrix (Fisher Scientific, Corning #356234) and injected into the right (GFP) and left (CNTF) axilla of 6-week-old female SCID mice, respectively. Perpendicular diameters of each tumor were measured with calipers. Tumor volume (TV) was calculated using the following formula: $TV=(width)^2 \times length/2$.

Statistical analysis

For in vitro and in vivo studies, the number of biological replicates was calculated using a statistical analysis for power determination. For all studies, we set an alpha value of 0.05, a power of 0.8, and a standard deviation of 0.25. For in vivo studies, we utilized the parameter of a 50% reduction in tumor volume to be considered a significant clinical response. For such studies, six-week-old female SCID mice were randomly assigned to experimental groups. Control and treated-tumor cells were injected into the right (GFP/control) and left (treatment/CNTF) axilla of the same mouse, respectively.

Statistical analysis was performed with one-way ANOVA (2 or more groups) and student's t test (2 groups) using the GraphPad Prism 6 software. The variance was similar between the groups that were statistically compared. Significance was defined as $p<0.05$. Data are shown as mean with the standard error of the mean (SEM), and images are representative of at least three biological replicates.

Supplementary Material

Refer to Web version on PubMed Central for supplementary material.

Acknowledgments

Financial support: UD and NH are supported by NIH grant R00CA143229 from the National Cancer Institute.

Reference

1. Blum R, Kloog Y. Metabolism addiction in pancreatic cancer. Cell Death Dis. 2014; 5:e1065. [PubMed: 24556680]
2. Chen J, Zhao S, Nakada K, Kuge Y, Tamaki N, Okada F, et al. Dominant-negative hypoxia-inducible factor-1 alpha reduces tumorigenicity of pancreatic cancer cells through the suppression of glucose metabolism. Am J Pathol. 2003; 162:1283–1291. [PubMed: 12651620]
3. Shang Y, Mao Y, Batson J, Scales SJ, Phillips G, Lackner MR, et al. Antixenograft tumor activity of a humanized anti-insulin-like growth factor-I receptor monoclonal antibody is associated with decreased AKT activation and glucose uptake. Mol Cancer Ther. 2008; 7:2599–2608. [PubMed: 18790743]
4. Walker-Samuel S, Ramasawmy R, Torrealdea F, Rega M, Rajkumar V, Johnson SP, et al. In vivo imaging of glucose uptake and metabolism in tumors. Nat Med. 2013; 19:1067–1072. [PubMed: 23832090]
5. Keshari KR, Sriram R, Koelsch BL, Van Criekinge M, Wilson DM, Kurhanewicz J, et al. Hyperpolarized 13C-pyruvate magnetic resonance reveals rapid lactate export in metastatic renal cell carcinomas. Cancer Res. 2013; 73:529–538. [PubMed: 23204238]
6. Andersson S, D'Arcy P, Larsson O, Sehat B. Focal adhesion kinase (FAK) activates and stabilizes IGF-1 receptor. Biochem Biophys Res Commun. 2009; 387:36–41. [PubMed: 19545541]
7. Arbet-Engels C, Janknecht R, Eckhart W. Role of focal adhesion kinase in MAP kinase activation by insulin-like growth factor-I or insulin. FEBS Lett. 1999; 454:252–256. [PubMed: 10431817]
8. Zheng D, Kurenova E, Ucar D, Golubovskaya V, Magis A, Ostrov D, et al. Targeting of the protein interaction site between FAK and IGF-1R. Biochem Biophys Res Commun. 2009; 388:301–305. [PubMed: 19664602]
9. Zhang J, Hochwald SN. The role of FAK in tumor metabolism and therapy. Pharmacol Ther. 2014; 142:154–163. [PubMed: 24333503]
10. Lim SK, Choi YW, Lim IK, Park TJ. BTG2 suppresses cancer cell migration through inhibition of Src-FAK signaling by downregulation of reactive oxygen species generation in mitochondria. Clin Exp Metastasis. 2012; 29:901–913. [PubMed: 22562501]
11. Zhang C, Lambert MP, Bunch C, Barber K, Wade WS, Krafft GA, et al. Focal adhesion kinase expressed by nerve cell lines shows increased tyrosine phosphorylation in response to Alzheimer's A beta peptide. J Biol Chem. 1994; 269:25247–25250. [PubMed: 7929215]
12. Zhu J, Wu YN, Zhang W, Zhang XM, Ding X, Li HQ, et al. Monocarboxylate transporter 4 facilitates cell proliferation and migration and is associated with poor prognosis in oral squamous cell carcinoma patients. PLoS One. 2014; 9:e87904. [PubMed: 24498219]
13. Lee HZ, Yeh FT, Wu CH. The effect of elevated extracellular glucose on adherens junction proteins in cultured rat heart endothelial cells. Life Sci. 2004; 74:2085–2096. [PubMed: 14969714]
14. Frame MC, Patel H, Serrels B, Lietha D, Eck MJ. The FERM domain: organizing the structure and function of FAK. Nat Rev Mol Cell Biol. 2010; 11:802–814. [PubMed: 20966971]
15. Doudna JA, Charpentier E. Genome editing. The new frontier of genome engineering with CRISPR-Cas9. Science. 2014; 346:1258096. [PubMed: 25430774]
16. Schultze A, Fiedler W. Clinical importance and potential use of small molecule inhibitors of focal adhesion kinase. Anticancer Agents Med Chem. 2011; 11:593–599. [PubMed: 21787277]
17. Tomaino B, Cappello P, Capello M, Fredolini C, Sperduti I, Migliorini P, et al. Circulating autoantibodies to phosphorylated alpha-enolase are a hallmark of pancreatic cancer. J Proteome Res. 2011; 10:105–112. [PubMed: 20455595]
18. Cui J, Shi M, Xie D, Wei D, Jia Z, Zheng S, et al. FOXM1 promotes the warburg effect and pancreatic cancer progression via transactivation of LDHA expression. Clin Cancer Res. 2014; 20:2595–2606. [PubMed: 24634381]

19. Christofk HR, Vander Heiden MG, Wu N, Asara JM, Cantley LC. Pyruvate kinase M2 is a phosphotyrosine-binding protein. Nature. 2008; 452:181–186. [PubMed: 18337815]
20. Santidrian AF, Matsuno-Yagi A, Ritland M, Seo BB, LeBoeuf SE, Gay LJ, et al. Mitochondrial complex I activity and NAD+/NADH balance regulate breast cancer progression. J Clin Invest. 2013; 123:1068–1081. [PubMed: 23426180]
21. Jones S, Zhang X, Parsons DW, Lin JC, Leary RJ, Angenendt P, et al. Core signaling pathways in human pancreatic cancers revealed by global genomic analyses. Science. 2008; 321:1801–1806. [PubMed: 18772397]
22. Jiao Y, Shi C, Edil BH, de Wilde RF, Klimstra DS, Maitra A, et al. DAXX/ATRX, MEN1, and mTOR pathway genes are frequently altered in pancreatic neuroendocrine tumors. Science. 2011; 331:1199–1203. [PubMed: 21252315]
23. Konstantinidou G, Ramadori G, Torti F, Kangasniemi K, Ramirez RE, Cai Y, et al. RHOA-FAK is a required signaling axis for the maintenance of KRAS-driven lung adenocarcinomas. Cancer Discov. 2013; 3:444–457. [PubMed: 23358651]
24. Hecker TP, Ding Q, Rege TA, Hanks SK, Gladson CL. Overexpression of FAK promotes Ras activity through the formation of a FAK/p120RasGAP complex in malignant astrocytoma cells. Oncogene. 2004; 23:3962–3971. [PubMed: 15077193]
25. Ward KK, Tancioni I, Lawson C, Miller NL, Jean C, Chen XL, et al. Inhibition of focal adhesion kinase (FAK) activity prevents anchorage-independent ovarian carcinoma cell growth and tumor progression. Clin Exp Metastasis. 2013; 30:579–594. [PubMed: 23275034]
26. Serrels A, McLeod K, Canel M, Kinnaird A, Graham K, Frame MC, et al. The role of focal adhesion kinase catalytic activity on the proliferation and migration of squamous cell carcinoma cells. Int J Cancer. 2012; 131:287–297. [PubMed: 21823119]
27. Muller G, Jung C, Wied S, Welte S, Frick W. Insulin-mimetic signaling by the sulfonylurea glimepiride and phosphoinositolglycans involves distinct mechanisms for redistribution of lipid raft components. Biochemistry. 2001; 40:14603–14620. [PubMed: 11724574]
28. Muller G, Wied S, Frick W. Cross talk of pp125(FAK) and pp59(Lyn) non-receptor tyrosine kinases to insulin-mimetic signaling in adipocytes. Mol Cell Biol. 2000; 20:4708–4723. [PubMed: 10848597]
29. Zheng D, Golubovskaya V, Kurenova E, Wood C, Massoll NA, Ostrov D, et al. A novel strategy to inhibit FAK and IGF-1R decreases growth of pancreatic cancer xenografts. Mol Carcinog. 2010; 49:200–209. [PubMed: 19885860]
30. Zhang J, He D, Zajac-Kaye M, Hochwald SN. A small molecule FAK kinase inhibitor, GSK2256098, inhibits growth and survival of pancreatic ductal adenocarcinoma cells. Cell Cycle. 2014
31. Lee SH, Lee YJ, Park SW, Kim HS, Han HJ. Caveolin-1 and integrin beta1 regulate embryonic stem cell proliferation via p38 MAPK and FAK in high glucose. J Cell Physiol. 2011; 226:1850–1859. [PubMed: 21506116]
32. Diaz-Ramos A, Roig-Borrellas A, Garcia-Melero A, Lopez-Alemany R. alpha-Enolase, a multifunctional protein: its role on pathophysiological situations. J Biomed Biotechnol. 2012; 2012:156795. [PubMed: 23118496]
33. Mikuriya K, Kuramitsu Y, Ryozawa S, Fujimoto M, Mori S, Oka M, et al. Expression of glycolytic enzymes is increased in pancreatic cancerous tissues as evidenced by proteomic profiling by two-dimensional electrophoresis and liquid chromatography-mass spectrometry/mass spectrometry. Int J Oncol. 2007; 30:849–855. [PubMed: 17332923]
34. Sudhakaran PR, Viji RI, Kiran MS, Sameer Kumar VB. Endothelial cell-laminin interaction: modulation of LDH expression involves alpha6beta4 integrin-FAK-p38MAPK pathway. Glycoconj J. 2009; 26:697–704. [PubMed: 18814027]
35. Tornatore TF, Dalla Costa AP, Clemente CF, Judice C, Rocco SA, Calegari VC, et al. A role for focal adhesion kinase in cardiac mitochondrial biogenesis induced by mechanical stress. Am J Physiol Heart Circ Physiol. 2011; 300:H902–912. [PubMed: 21148763]
36. Peng X, Kraus MS, Wei H, Shen TL, Pariaut R, Alcaraz A, et al. Inactivation of focal adhesion kinase in cardiomyocytes promotes eccentric cardiac hypertrophy and fibrosis in mice. J Clin Invest. 2006; 116:217–227. [PubMed: 16374517]

37. Ucar DA, Magis AT, He DH, Lawrence NJ, Sebti SM, Kurenova E, et al. Inhibiting the Interaction of cMET and IGF-1R with FAK Effectively Reduces Growth of Pancreatic Cancer Cells in vitro and in vivo. Anticancer Agents Med Chem. 2013; 13:595–602. [PubMed: 23272972]

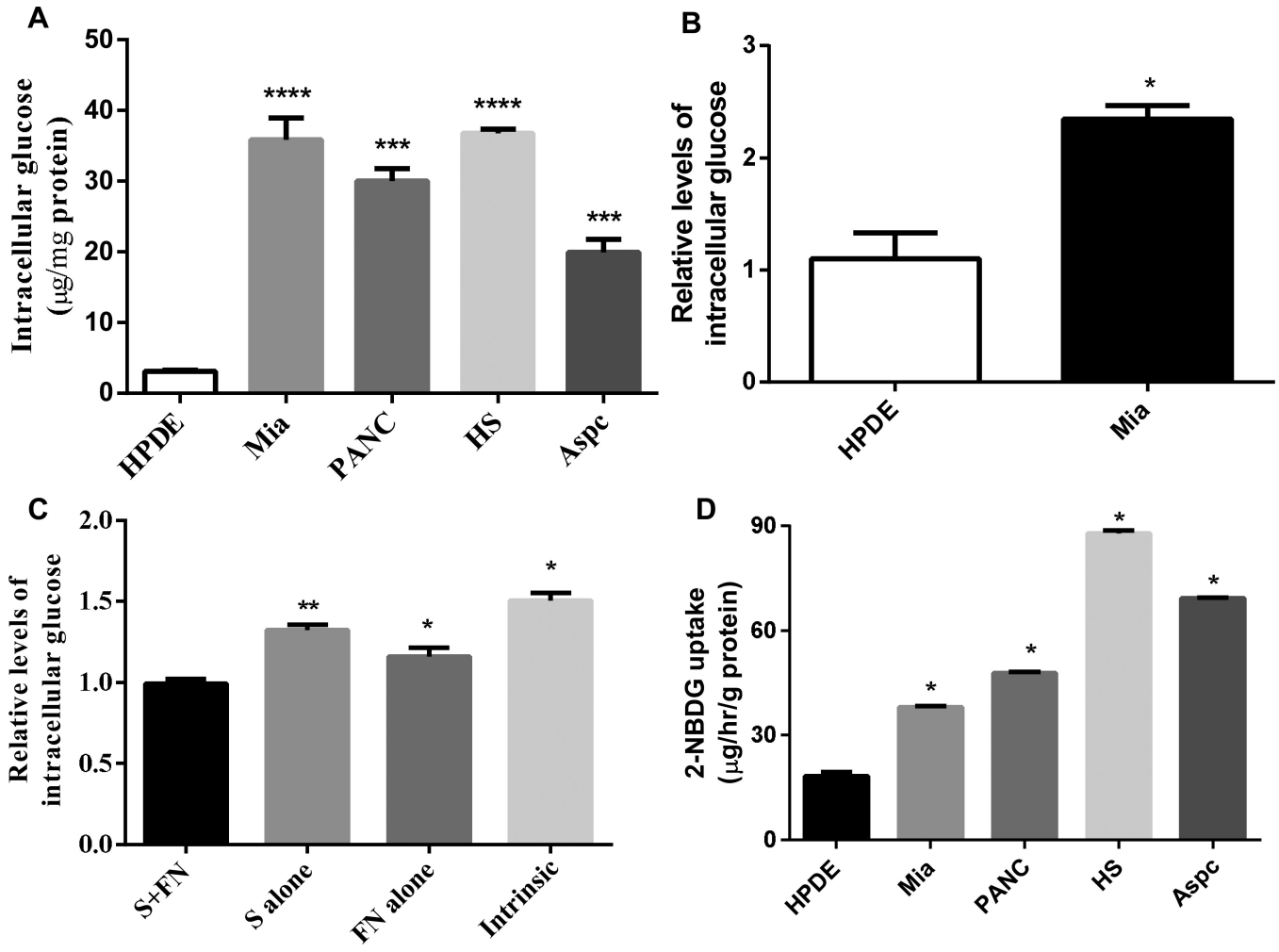

Fig 1. Intrinsic factor modulation of glucose elevation in pancreatic tumor cells

A. HPDE and PDAC (Miapaca-2, Panc-1, HS766T and Aspc-1) were cultured on a fibronectin-coated low binding 6-well plate for 48 hr. Attached cells were harvested and subjected to Amplex Red glucose assay (Invitrogen). Glucose levels were normalized to cellular protein levels (μg glucose/mg protein). Data are averages with SEM from 9 biological replicates. ***: $p<0.001$ vs HPDE, and ****: $p<0.0001$ vs HPDE. **B.** HPDE and Miapaca-2 cells were kept in medium containing 4.5 g/l of glucose for 48 hr. Glucose contents in cell lysates were determined and normalized to cellular protein levels, and the relative level of intracellular glucose in Miapaca-2 was normalized to that in HPDE cells for comparison. Data are averages with SEM from 3 biological replicates.*: $p<0.05\%$ vs HPDE. **C.** The effects of growth factor and anchorage stimulation on intracellular glucose levels. The relative levels of intracellular glucose in Miapaca-2 under anchorage- and/or growth factor-limited conditions were normalized to that under normal (with anchorage and growth factor stimulation). S: 10% Serum, FN: Fibronectin-coated plate, and Intrinsic: 0.5% serum and no FN-coating. Data are averages with SEM from 3 biological replicates.*: $p<0.05\%$ vs S+FN, and **: $p< 0.01$ vs S+FN. **D.** The effects of intrinsic factors on glucose influx. Equal numbers of HPDE and PDAC cells in depleted DMEM medium (containing 2-NBDG, but without FBS, glucose, pyruvate, and glutamine) were placed in the low cell binding wells

and incubated for 2 hr. Fluorescence intensities of cellular 2-NBDG were normalized to protein contents in the cell lysates. Data are averages with SEM from 3 replicates.*: $p<0.01\%$ vs HPDE.

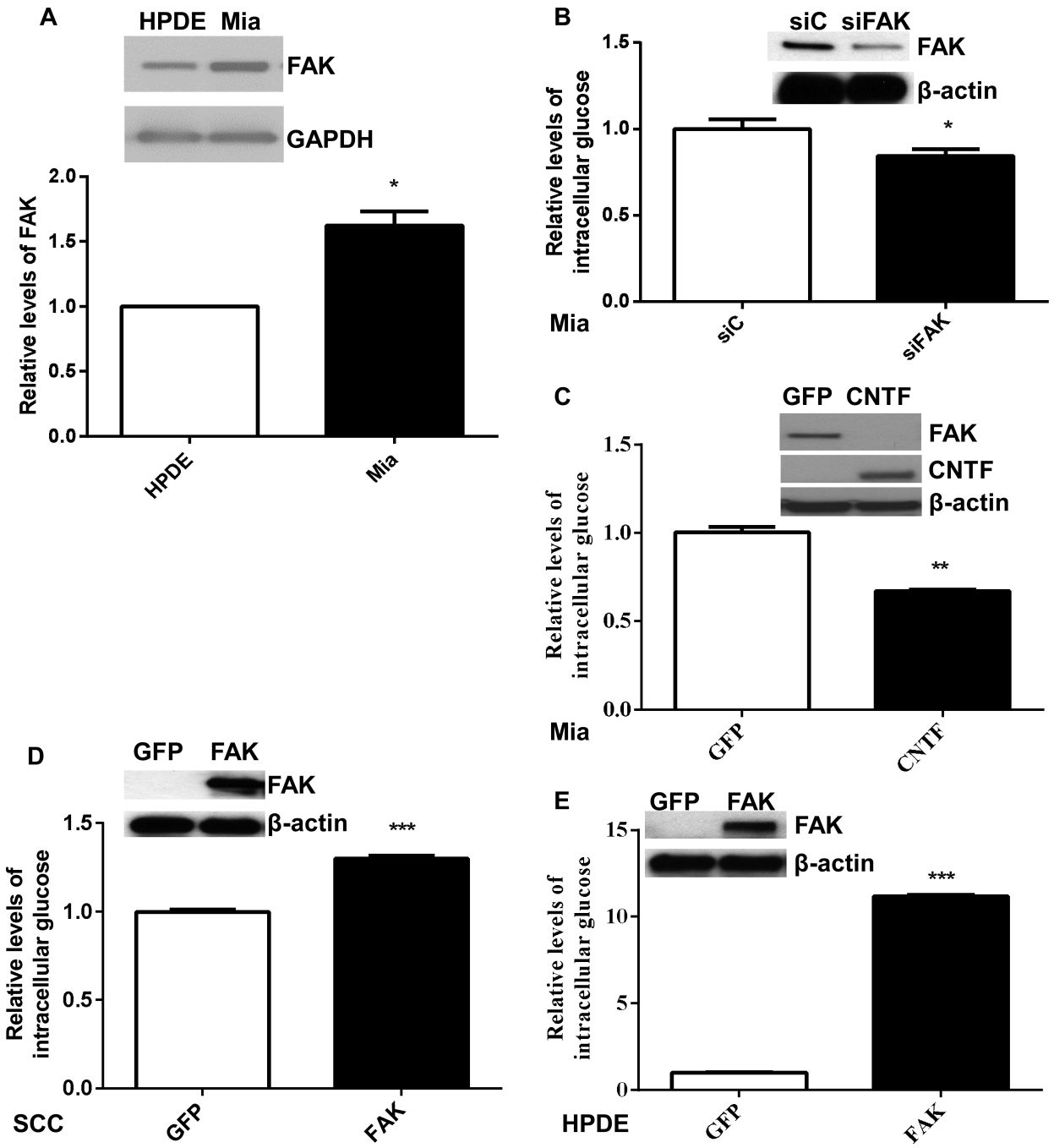

Fig 2. FAK modulation of intrinsic glucose elevation

A. The levels of FAK protein were assessed using Western blot analysis. The band intensity of total FAK (representative images, insets) was determined using Image-J and normalized to that of GAPDH. The relative levels of FAK in Miapaca-2 (Mia) were calculated and statistically analyzed. Data are averages with SEM from 6 biological replicates.*: $p<0.05$ vs HPDE. **B.** siRNA inhibition of FAK decreases intrinsic elevation of intracellular glucose. Control (siC) and FAK siRNA (siFAK)-transfected Miapaca-2 cells were cultured under extracellular stimulus-limited conditions and subjected to glucose assay. The level of

intracellular glucose in siFAK-treated cells was normalized to cellular protein levels and then to the glucose level in siC cells. Data are averages with SEM from 3 biological replicates.*: $p<0.05$ vs siC. **C.** CNTF (a dominant-negative form of FAK) inhibition of FAK expression decreases intracellular glucose levels. The relative levels of total FAK in Miapaca-2 cells transfected with pGFP or pCNTF (the MW of mCherry+FAK F1 subdomain: ~45 kDa) were assessed (insets). The stable transfected cells were cultured under stimulus-limited conditions and subjected to glucose analysis. The level of intracellular glucose in pCNTF-transfected cells was normalized to cellular protein levels and then to the glucose level in pGFP-transfected cells. GFP: Cells expressing the *GFP* gene, and CNTF: Cells expressing the N-terminal *FAK* gene. Data are averages with SEM from 3 biological replicates. **: $p<0.01$ vs GFP. **D.** FAK expression was reinstated in FAK null SCC cells by ectopic transfection of FAK deficient cells with pcFAK vectors. The FAK-restored cells were cultured on a FN-coated low cell binding plate and assessed for glucose levels. The level of intracellular glucose in pcFAK-transfected cells was normalized to cellular protein levels and then to the glucose level in pGFP-transfected cells. GFP: Cells expressing the *GFP* gene, and FAK: Cells expressing the mCherry-tagged *FAK* gene. Data are averages with SEM from 3 biological replicates.***: $p<0.001$ vs control. **E.** HPDE cells were transfected with pGFP or pcFAK constructs, kept under stimulus-limited conditions for 72 hr, and subjected to glucose and protein analysis. The level of intracellular glucose in pcFAK-transfected cells was normalized to cellular protein levels and then to the glucose level in pGFP-transfected cells. GFP: Cells expressing the *GFP* gene, and FAK: Cells expressing the mCherry-tagged *FAK* gene. Data are averages with SEM from 3 biological replicates. ***: $p<0.001$ vs control.

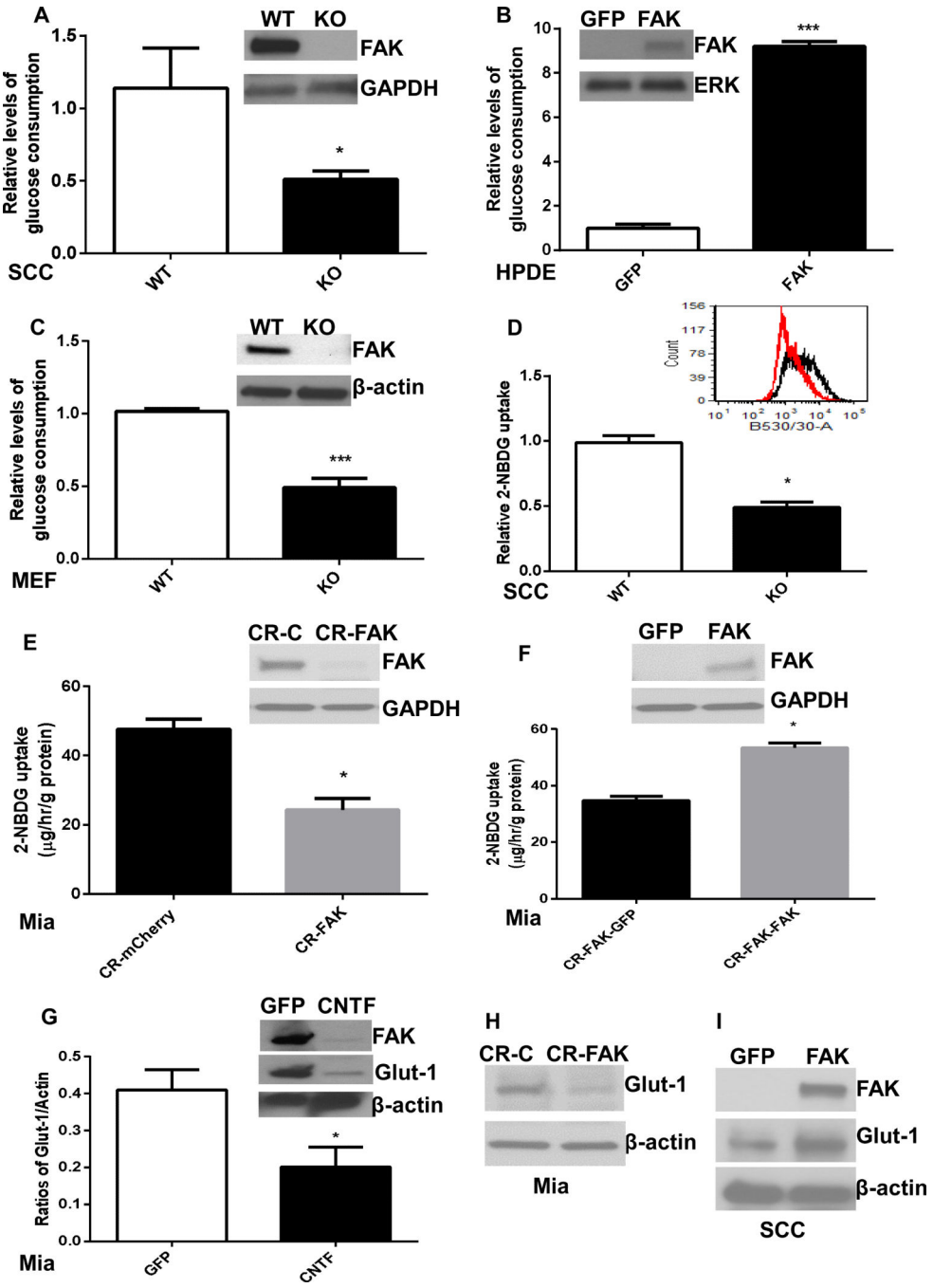

Fig 3. FAK promotes glucose consumption and uptake

A. Wild-type (WT) and *FAK* null (KO) SCC cells were used as to examine the effects of FAK on glucose consumption. The levels of glucose in medium incubated with WT or *FAK* KO cells were determined. Glucose consumption was calculated (μg glucose/hr/mg protein). Then, the values were normalized to controls and shown as relative levels of glucose consumption. Data are averages with SEM from 6 biological replicates.*: $p < 0.05$ vs WT. **B.** HPDE cells were transfected with pGFP or pcFAK constructs, incubated for 56 hr, and subjected to glucose analysis. The amount of glucose used by pcFAK-transfected cells was

normalized to cellular protein levels and then to that by pGFP-transfected cells. GFP: Cells expressing the *GFP* gene, and FAK: Cells expressing the mCherry-tagged *FAK* gene. Data are averages with SEM from 3 biological replicates. ****: p<0.0001 vs GFP. **C.** FAK expression contributes to increased glucose consumption in metabolically active normal cells. WT and *FAK* null MEF (KO) cells were subjected to glucose consumption analysis. The relative amount of glucose used by *FAK* KO cells was normalized to cellular protein levels and then to that by WT FAK cells. Data are averages with SEM from 6 biological replicates. ***: p<0.001 vs WT. **D.** FAK expression is correlated with glucose uptake. WT and *FAK* KO MEF cells were cultured in DMEM medium containing the fluorescence-tagged glucose (2-NBDG) and subjected to flow cytometry analysis. The representative histogram of 2-NBDG levels in the WT (in black) and *FAK* KO (in red) cells were shown as insets. Arithmetric means of 2-NBDG incorporation were calculated. Data are averages with SEM from 3 biological replicates. *: p<0.05 vs WT. **E.** Disruption of the *FAK* gene in Miapaca-2 cells using CRISPR-Cas9 vectors and assessment of glucose uptake. The amounts of 2-NBDG taken up by WT (CR-mCherry) and FAK deficient (CR-FAK) Miapaca-2 cells were assessed and expressed as μg 2-NBDG/hour/gram cellular protein. CR-C: Cells expressing the *mCherry* gene, and CRFAK: Cells transfected with the CRISPR-Cas9 vector targeting the *FAK* gene. Data are averages with SEM from 4 replicates.*: p<0.001 vs WT. **F.** The effects of reinstated FAK expression on glucose uptake. The FAK deficient Miapaca-2 cells were transfected with pGFP or pcFAK vectors and assessed for glucose uptake using 2-NBDG assays. GFP: Cells expressing the *GFP* gene (GFP), and FAK: Cells expressing the *mCherry-tagged FAK* (FAK) gene. Data are averages with SEM from 3 replicates. *: p<0.001 vs WT. **G.** The levels of Glut-1 protein in pGFP- or pCNTF-transfected Miapaca-2 cells were determined using Western blot analysis (representative images, insets). Image-J was used to assess band intensities. The intensity ratios of Glut-1/β-actin were calculated and statistically analyzed (Prism). GFP: Cells transfected with vehicles (pGFP), and CNTF: Cells transfected with the pCNTF vectors. Data are averages with SEM from 4 biological replicates.*: p<0.05 vs GFP. **H.** CRISPR-Cas9 FAK-mediated disruption of FAK expression leads to decreased levels of Glut1 protein in Miapaca-2 cells. **I.** Assessments of Glut-1 protein levels in pGFP- or pcFAK-transfected FAK KO SCC cells.

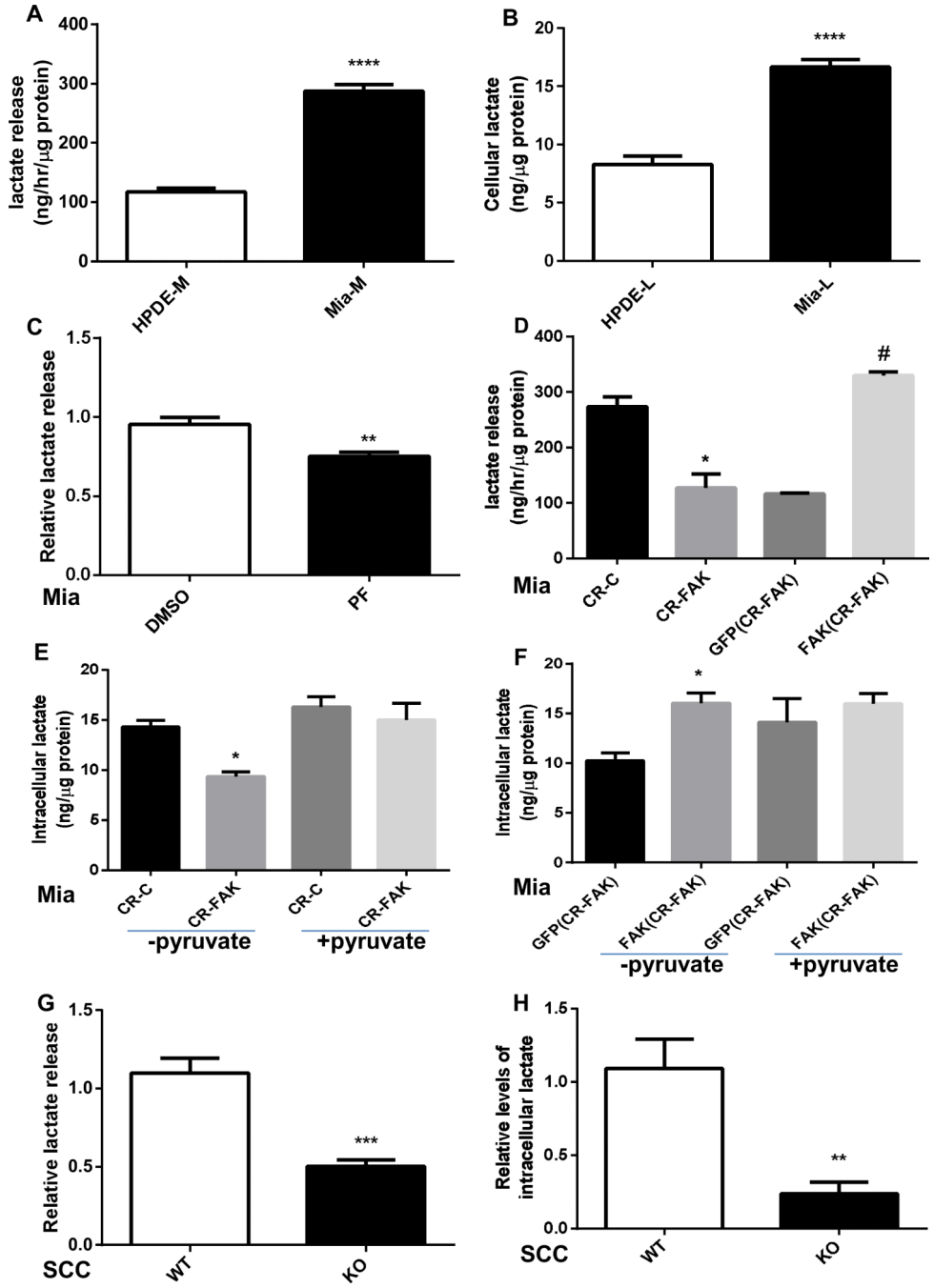

Figure 0004

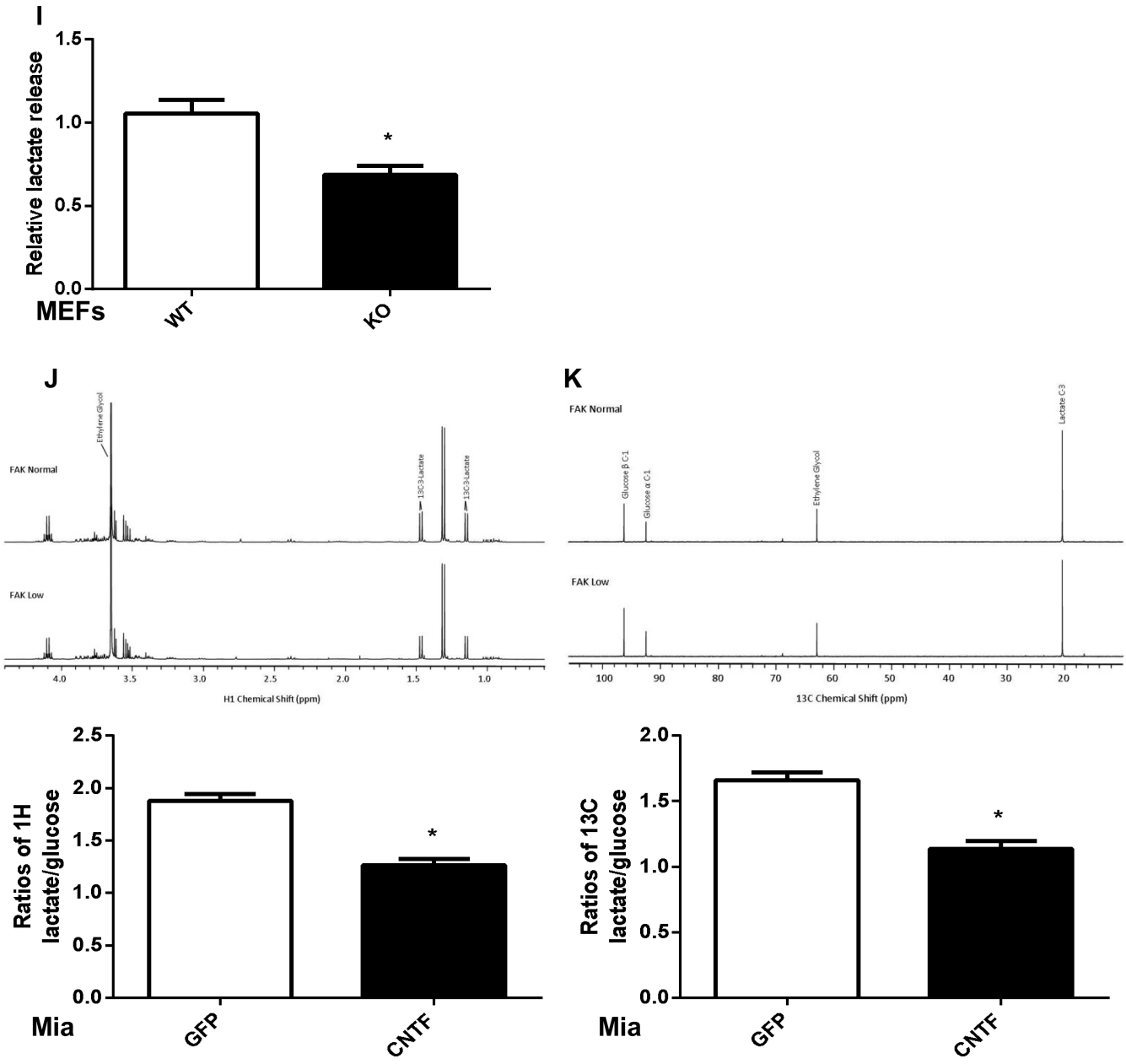

Figure 0005

Fig 4. FAK promotes lactate production

A. Miapaca-2 and HPDE cells were cultured in the medium containing the same amount of glucose and on a fibronectin-coated low binding plate for 24 hr. Lactate levels in the medium were measured, normalized to cellular protein levels and expressed as ng lactate released/hr/μg protein. Data are averages with SEM from 3 biological replicates. ****: $p<0.0001$ vs HPDE. **B.** Cell lysates derived from Miapaca-2 and HPDE were analyzed for lactate content, normalized to protein amount, and expressed as ng lactate/μg protein. Data are averages with SEM from 3 biological replicates. ****: $p<0.0001$ vs HPDE. **C.** Miapaca-2 cells (Mia) were cultured in medium containing 2 μM of the specific FAK inhibitor PF4554878 or DMSO for

48 hr and assessed for lactate release. The relative level of lactate released to the medium by PF-treated cells was normalized to cellular protein levels and then to that by vehicle-treated cells. Data are averages with SEM from 5 biological replicates.**: p<0.01 vs DMSO-treated cells. **D.** Lactate release of CRISPR-Cas9 FAK-disrupted and pcFAK-transfected Miapaca-2 cells were assessed. CR-C: Cells expressing the *mCherry* gene, CR-FAK: Cells transfected with the CRISPR-Cas9 vector targeting the *FAK* gene, GFP (CR-FAK): FAK deficient cells expressing the *GFP* gene (GFP), and FAK (CR-FAK): FAK deficient cells expressing the *mCherry-tagged FAK* (FAK) gene. Data are averages with SEM from 3 replicates.*: p<0.01 vs CR-C; and #: p<0.01 vs GFP (CR-FAK). **E and F.** Control (CR-C), FAK deficient (CR-FAK) Miapaca-2 cells and pGFP (GFP)-/pcFAK (FAK)-transfected CR-FAK cells were cultured in pyruvate-free medium (−pyruvate) for 24 hr and then in medium containing pyruvate (+pyruvate) for 24 hr to rescue FAK-reduced glycolysis. Intracellular lactate levels were measured and normalized to protein content. GFP (CR-FAK): FAK deficient cells expressing the *GFP* gene (GFP), and FAK (CR-FAK): FAK deficient cells expressing the *mCherry-tagged FAK* (FAK) gene. Data are averages with SEM from 3 replicates.*: p<0.01 vs CR-C or GFP (CR-FAK). **G and H.** Disruption of the *FAK* gene in SCC cells decreases lactate release and intracellular lactate levels. The relative levels of lactate release and intracellular lactate in *FAK* KO cells was normalized to cellular protein levels and then to that in WT *FAK* cells. Data are averages with SEM from 3 biological replicates.**: p<0.01 vs WT cells. **I.** Disrupting the FAK gene in MEFs leads to a lactate decline. The relative level of lactate released to the medium by *FAK* KO cells was normalized to cellular protein levels and then to that by WT *FAK* cells. Data are averages with SEM from 3 biological replicates.**: p<0.05 vs WT cells. **J and K.** NMR analysis of FAK-modulated glucose-to-lactate conversion. Miapaca-2 cells expressing the *GFP* or the *CNTF* gene were incubated in DMEM containing 4.5 g/l of ^{13}Carbon-labeled glucose for 24 hr. ^{1}H (panel J) or ^{13}C (panel K) lactate was analyzed using NMR (upper panels). The representatives of ^{1}H (upper panel J) and ^{13}C (upper panel K) lactate profiles of NMR were shown. The relative levels of ^{1}H/^{13}C lactate and glucose were determined using ethylene glycol as an internal reference. The ratios of labeled lactate and glucose were calculated (lower panels). Data are averages with SEM from 3 replicates.**: p<0.05 vs GFP-transfected cells.

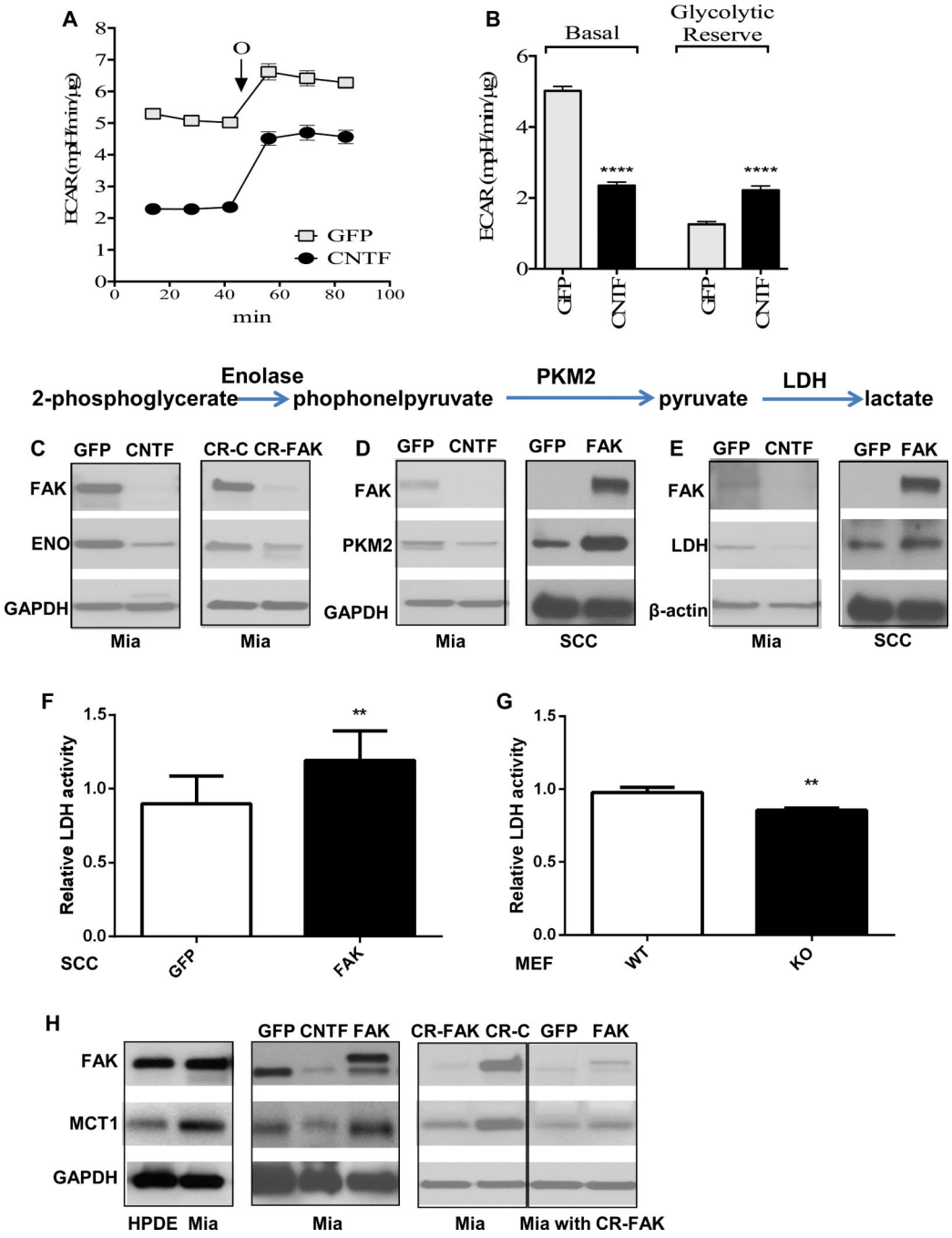

Fig 5. FAK-promoted glycolysis is associated with increases in key regulatory proteins

A. ECAR of GFP- and CNTF-transfected Miapaca-2 cells. Oligomycin A (O; 1mM) was administered to inhibit mitochondrial respiration and induce maximal glycolytic flux. **B.** Basal glycolysis decreases in cells expressing the *CNTF* gene. Glycolytic reserve: the difference between Oligomycin A induced ECAR and basal ECAR. Data are averages with SEM from 3 biological replicates. ****: $p<0.001$ vs GFP-transfected cells. **C.** CNTF- (the left panel) and CRISPR-Cas9-FAK-(the right panel) decreased levels of ENO protein in Miapaca-2 cells. GFP: Cells transfected with vehicle (pGFP), CNTF: Cells transfected with

the pCNTF vectors, CR-C: Cells expressing the *mCherry* gene, and CR-FAK: Cells transfected with the pCRISPR-Cas9 vector targeting the *FAK* gene. **D.** CNTF suppression of FAK decreases the levels of PKM2 protein in Miapaca-2 cells (the left panel), and ectopic expression of FAK in *FAK* KO SCC cells increases PKM2 protein mass (the right panel). GFP: Cells transfected with vehicles (GFP), CNTF: Cells transfected with the pCNTF vectors, and FAK: Cells expressing the *FAK* gene. **E.** CNTF inhibition of FAK results in decreased levels of LDH protein in Miapaca-2 cells (the left panel). Ectopic expression of FAK in *FAK* KO SCC cells increases the level of LDH protein (the right panel). GFP: Cells transfected with vehicles (pGFP), CNTF: Cells transfected with the pCNTF vectors, and FAK: Cells expressing the *FAK* gene. **F.** Restoring FAK expression increases LDH activity in *FAK* KO SCC cells during unfavorable conditions. LDH activity in cell homogenates was normalized to protein levels and the GFP-transfected control. GFP: Cells transfected with vehicles (pGFP), and FAK: Cells expressing the *FAK* gene. Data are averages with SEM from 3 biological replicates. **p<0.01 vs GFP. **G.** WT and *FAK* KO MEFs were cultured on the FN-coated plate and kept in DMEM medium containing 0.5% FBS for 48 hr. LDH activity in cell homogenates was determined, normalized to protein levels, and the GFP-transfected control. Data are averages with SEM from 3 biological replicates. **p<0.01 vs WT. **H.** FAK expression is correlated with MCT1 levels in HPDE and Miapaca-2 (Mia) cells (the left panel). CNTF inhibition of FAK expression decreases the MCT1 level, and ectopic expression of FAK increases MCT1 protein mass (the middle panel). CRISPR-Cas9 disruption of FAK expression decreases and ectopic restoration of FAK expression increases MCT levels in Miapaca-2 cells (the right panel). GFP: Cells transfected with vehicles (pGFP), CNTF: Cells transfected with the pCNTF vectors, FAK: Cells expressing the *FAK* gene, CR-FAK: Cells transfected with the pCRISPR-Cas9 vector targeting the *FAK* gene, and CR-C: Cells expressing the *mCherry* gene.

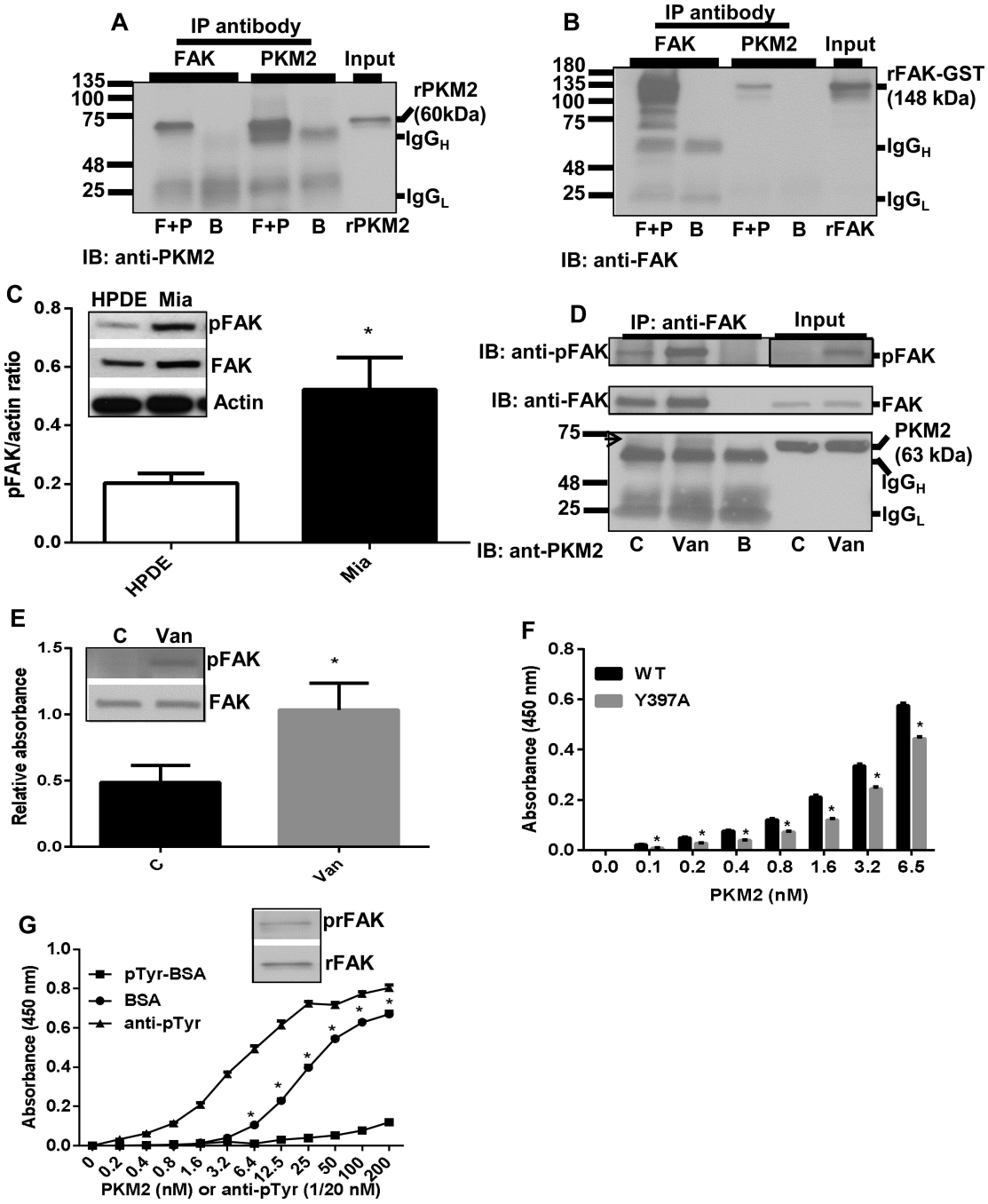

Fig 6. FAK directly binds to PKM2

A. Purified phospho-Y397 FAK (GST-tagged rFAK, MW=148 kDa) and active rPKM2 (1-531 aa + NT His-Tag, MW=60.1 kDa) were mixed in the binding buffer, immunoprecipitated using an anti-FAK (the left side of the image) or anti-PKM2 (the right side of the image) antibody, fractionated on a SDS-PAGE gel and immuno-detected using an anti-PKM2 antibody. IP: Immunoprecipitation; IB: Western blot analysis; rPKM2: recombinant PKM2; rFAK: recombinant FAK; F: rFAK; P: rPKM2; B: blank; F+P: rFAK mixed with rPKM2; and IgG-h/l: immunoglobulin heavy/light chain. **B.** The same

membrane was stripped and reprobed using an anti-FAK antibody to detect the FAK levels in the anti-FAK (the left side of the image) or anti-PKM2 (the right side of the image) antibody-immunoprecipitated complexes. **C.** The band intensity of phosphor- and total FAK (insets) was determined (Image-J), normalized to that of actin, and significance was analyzed (Prism). Data are averages with SEM from 4 biological replicates. *: $p<0.05$ vs HPDE. **D.** Tyrosine phosphorylation enhances PKM2 binding. Miapaca-2 cells were incubated with the vehicle (C) or pervanadate (Van), a potent phosphotyrosine phosphatase inhibitor. IP/Western blot analysis (IB) was performed to examine the effects of FAK Y397 phosphorylation on FAK-PKM2 interaction. **E.** Vehicle (C)- or pervanadate (Van)-treated cell lysates were immobilized, and their binding with PKM2 was immune-detected using the anti-PKM2 antibody. Data are averages with SEM from 4 biological replicates.*: $p<0.05$ vs vehicle-treated cells. **F.** WT or mutated FAK Y397A was coated on the plate. PKM2 binding to the immobilized FAK protein was immunodetected using the anti-PKM2 antibody. Data are averages with SEM from 3 replicates.*: $p<0.05$ vs WT rFAK. **G.** Phosphorylated rFAK (insets) was immobilized on a 96-well plate. Purified active PKM2 (0-200 nM) or an anti-phosphotyrosine (pTyr, 0-10 nM) antibody was added to the FAK-coated wells, rinsed and immuno-detected using an anti-PKM2 antibody or secondary antibody. Phosphotyrosine-BSA (pTyr-BSA) was used to block the interaction between PKM2 and phosphorylated/active FAK. Data are averages with SEM from 3 replicates.*: $p<0.05$ vs pTyr-BSA.

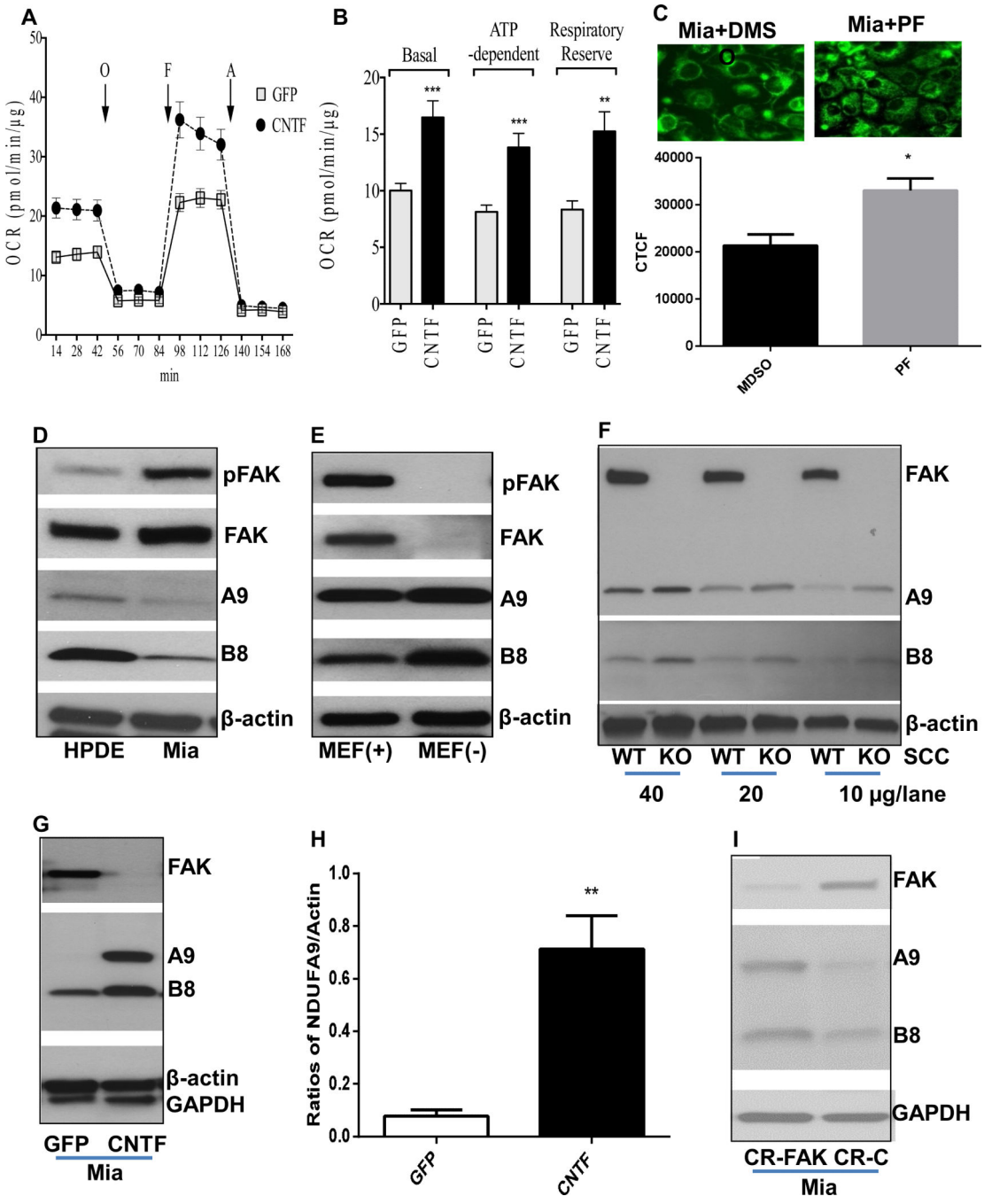

Fig 7. FAK-decreased mitochondrial respiration and complex I subunits

A. OCR of Miapaca-2 cells expressing the *GFP* or *CNTF* gene. **B.** Basal OCR, ATP dependent OCR (difference between basal OCR and Oligomycin A (O) inhibited OCR), and maximal FCCP (F)-induced OCR. Data are averages with SEM from 3 biological replicates. **p<0.01 vs GFP, ***p< 0.001 vs GFP, ****p<0.0001 vs GFP. **C.** MitoTracker green dye was used to assess PF4554878 (PF) or DMSO-altered distribution of functional mitochondria in live Miapaca-2 cells. Image-J was used to quantify mitochondrial fluorescence intensity. The corrected total cell fluorescence (CTCF) was calculated using the

formula: Integrated Density – (Area of selected cell X Mean fluorescence of background readings). Data are averages with SEM from 6 biological replicates.*: p<0.01 vs DMSO. **D.** NDUFA9 and NDUFB8 levels in HPDE and Miapaca-2 cells. **E.** Interruption of the *FAK* gene increases NDUFA9 and NDUFB8 protein in MEFs. **F.** FAK deficiency leads to increased NDUFA9 and NDUFB8 levels in *FAK* KO SCC cells. Varied amounts of protein were loaded to verify the altered levels of NDUF A9 (A9) and NDUF B8 (B8). **G.** CNTF inhibition of FAK in Miapaca-2 cells and Western blot analysis of DNUF A9 (A9) and DNUFB8 (B8) levels in Miapaca-2 cells. **H.** Densitometric analysis of NDUF A9 levels in GFP- and CNTF-transfected cells. Band intensities were determined (Image-J) and analyzed (Prism). Data are averages with SEM from 3 replicates.**: p< 0.01 vs GFP. **I.** CRISPR-Cas9 FAK interruption of the *FAK* gene in Miapaca-2 cells leads to increased levels of NDUFA9 and NDUFB8 protein.

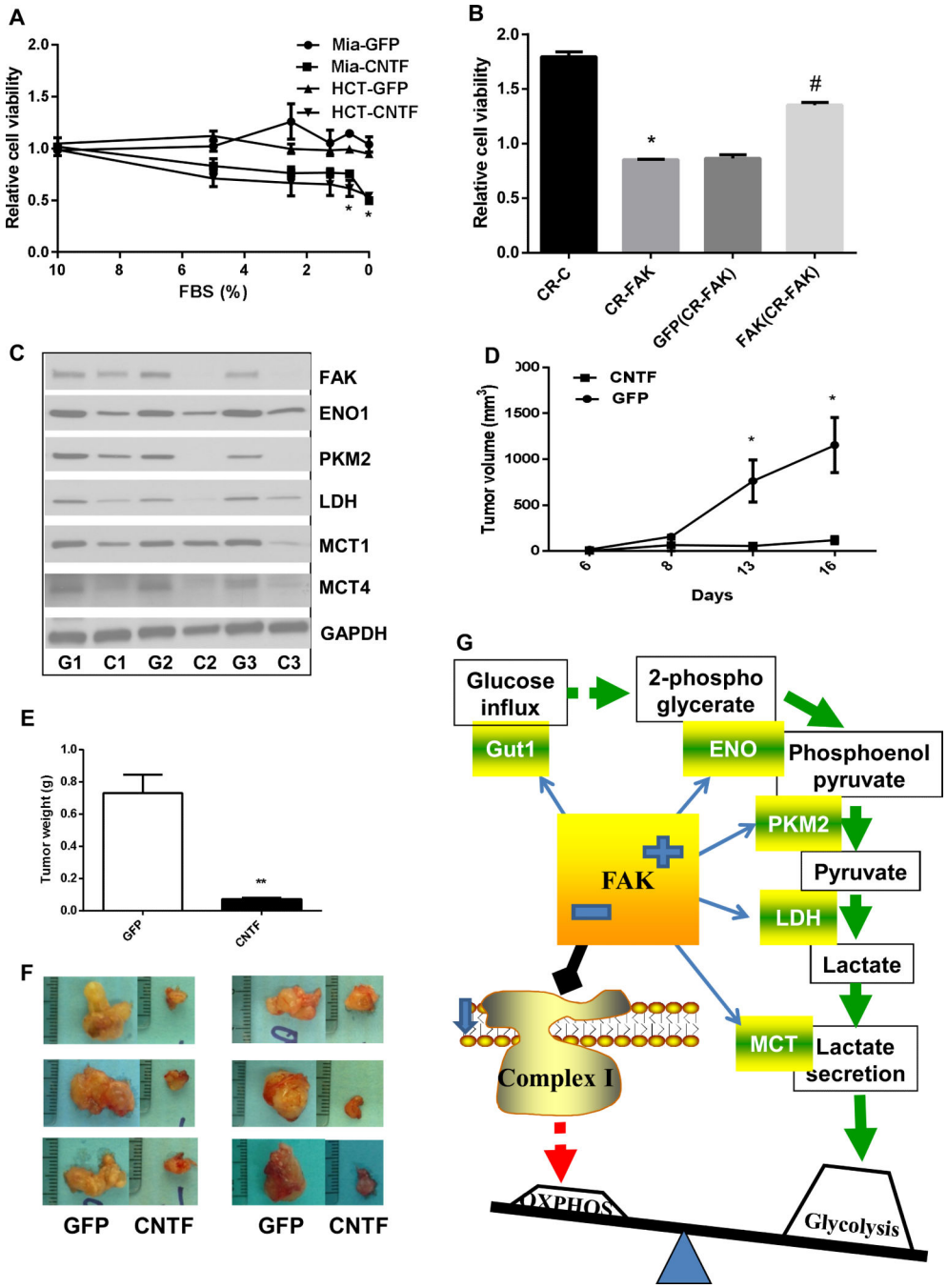

Fig 8. Attenuation of FAK-promoted oncometabolism restores growth factor-dependency and reduces tumorigenicity

A. CNTF inhibition of FAK expression re-sensitizes tumor cells to growth factor withdrawal-decreased cell viability. Miapaca-2 or HCT116 cells expressing the *GFP* or *CNTF* gene were cultured in medium containing 0-10% FBS for 24 hr and subjected to WST-1 cell viability assessed. O.D. values were normalized to that of cells in 10% FBS. Mia-GFP: Miapaca-2 cells transfected with the pGFP vector; Mia-CNTF: Miapaca-2 cells transfected with pcFAK constructs; HCT-GFP: HCT116 cells transfected with the pGFP vector; and HCT-CNTF: HCT116 cells transfected with pcFAK constructs. Data are

averages with SEM from 3 replicates. *: p< 0.05 vs GFP. **B.** CRISPR-Cas9 FAK and pcFAK-transfected Miapaca-2 cells were cultured under growth factor and anchorage-limited conditions for 24 hr and subjected to cell viability assay using WST-1. OD values of the cells incubated for 24 hr was normalized to those of respective cells kept for 0 hr. CR-C: Cells expressing the *mCherry* gene, CR-FAK: Cells transfected with the CRISPR-Cas9 vector targeting the *FAK* gene, GFP (CR-FAK): FAK deficient cells transfected with vehicles (pGFP), and FAK (CR-FAK): FAK deficient cells transfected with pcFAK vectors. Data are averages with SEM from 3 replicates. *: p< 0.05 vs CR-C, and #: p<0.05 vs GFP (CR-FAK). **C.** GFP- or CNTF-transfected HCT116 cells were injected into SCID mice. The protein levels of FAK, ENO1, PKM2, LDH, and MCT in xenografts were assessed. G1-G3: GFP-transfected xenografts; and C1-C3: CNTF-transfected xenografts. **D.** Sizes of GFP- and CNTF-transfected xenografts. Data are averages with SEM from 6 biological replicates.*: p< 0.05 vs GFP. **E.** Weights of tumors derived from GFP- or CNTF-transfected HCT116 cells. Data are averages with SEM from 6 biological replicates. **: p< 0.01 vs GFP. **F.** Images of isolated xenografts derived from GFP- or CNTF-transfected cells. **G.** FAK modulation of glucose oncometabolism. FAK increases glucose influx and the protein levels of Glut1, ENO1, PKM2, LDH and MCT, leading to enhanced glycolysis. On the other hand, FAK decreases complex I subunit mass and OXPHOS. This triggers the shift of the OXPHOS/glycolysis balance to aerobic glycolysis.